DE LA RECHERCHE À L'INDUSTRIE

Ph.D. defense

High-order cell-centered discontinuous Galerkin discretizations for scalar conservation laws and Lagrangian hydrodynamics

CEA CESTA[1] and INRIA[2] | F. Vilar[1], P.-H. Maire[1], R. Abgrall[2]

16 NOVEMBER 2012

www.cea.fr

Content

1 Introduction and preliminary results

2 2D Lagrangian hydrodynamics

3 DG discretization general framework

4 Second-order DG scheme

5 Third-order DG scheme

6 Conclusions and perspectives

Content

1 Introduction and preliminary results

2 2D Lagrangian hydrodynamics

3 DG discretization general framework

4 Second-order DG scheme

5 Third-order DG scheme

6 Conclusions and perspectives

Motivations and methodology

Motivations

- Inertial confinement fusion $\longrightarrow$ compressible gas dynamics simulation
- Complex flows (very intense shock and rarefaction waves, strong variation of the fluid domain, multimaterial flows, high cell aspect ratios)
- Lagrangian formalism (reference frame moving with the fluid)
- Very high-order extension of the Finite Volume EUCCLHYD scheme

P.-H. Maire, R. Abgrall, J. Breil and J. Ovadia, *A cell-centered Lagrangian scheme for two-dimensional compressible flow problems.* SIAM J. Sci. Comput., 2007.

Progressive methodology

- **1D scalar conservation laws** DG discretization
- **2D scalar conservation laws** on unstructured grids DG discretization
- **1D system of conservation laws** DG discretization
- **2D gas dynamics equation** written in a total Lagrangian formalism, on total unstructured grids DG discretization

Discontinuous Galerkin (DG)

DG schemes

- Natural extension of Finite Volume method
- Piecewise polynomial approximation of the solution in the cells
- High-order scheme to achieve high accuracy

Procedure

- Local variational formulation
- Choice of the numerical fluxes (global L^2 stability, entropy inequality)
- Time discretization - TVD multistep Runge-Kutta

  C.-W. SHU, *Discontinuous Galerkin methods: General approach and stability.* 2008.

- Limitation - vertex-based hierarchical slope limiters

  D. KUZMIN, *A vertex-based hierarchical slope limiter for p-adaptive discontinuous Galerkin methods.* J. Comp. Appl. Math., 2009.

Comparison between DG schemes with limitation

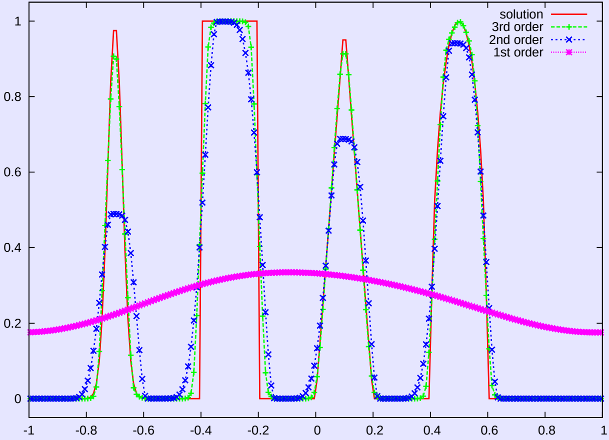

FIGURE: 1D linear advection of a combination of smooth and discontinuous profiles after 10 periods using 200 cells.

SCL on an unstructured grid made of 2500 **polygonal cells**

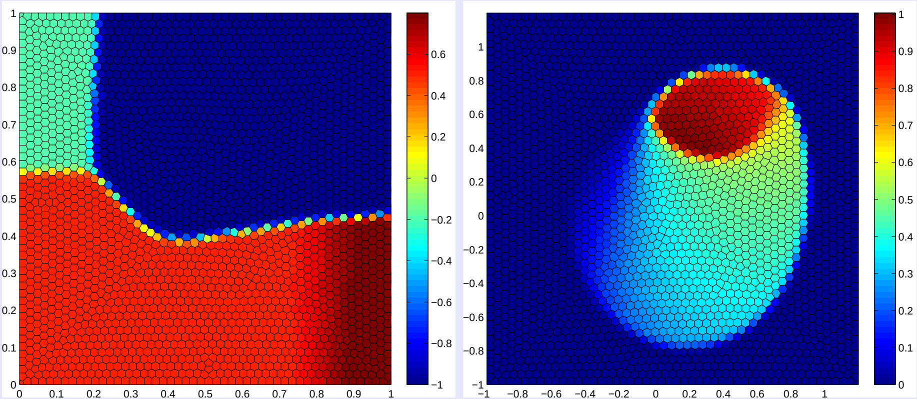

(a) Burgers problem. (b) Buckley-Leverett problem.

FIGURE: Numerical solutions using third-order DG scheme with limitation.

J.-L. GUERMOND, R. PASQUETTI AND B. POPOV, *Entropy viscosity method for non-linear conservation laws.* J. Comp. Phys., 2011.

2D Scalar Conservation Laws (SCL)

Third-order DG scheme without limitation

	L_1		L_2		L_∞	
$\mathcal{N}_c$	E_{L_1}	q_{L_1}	E_{L_2}	q_{L_2}	E_{L_∞}	q_{L_∞}
10×10	1.96E-3	3.14	2.55E-3	3.09	8.07E-3	2.90
20×20	2.22E-4	3.01	3.00E-4	3.01	1.08E-3	3.02
40×40	2.75E-5	3.00	3.73E-5	3.00	1.33E-4	3.01
80×80	3.43E-6	3.00	4.67E-6	3.00	1.65E-5	3.01
160×160	4.29E-7	-	5.83E-7	-	2.05E-6	-

TABLE: Rate of convergence in the case of the linear advection ($\boldsymbol{A} = (1,1)^t$) of the smooth initial condition $u^0(\boldsymbol{x}) = \sin(2\pi x)\sin(2\pi y)$ where $\boldsymbol{x} = (x,y)^t \in [0,1]^2$, with periodic boundary conditions, at the end of a period on Cartesian grids with a CFL$= 0.1$.

1D Lagrangian gas dynamics

Third-order DG scheme without limitation

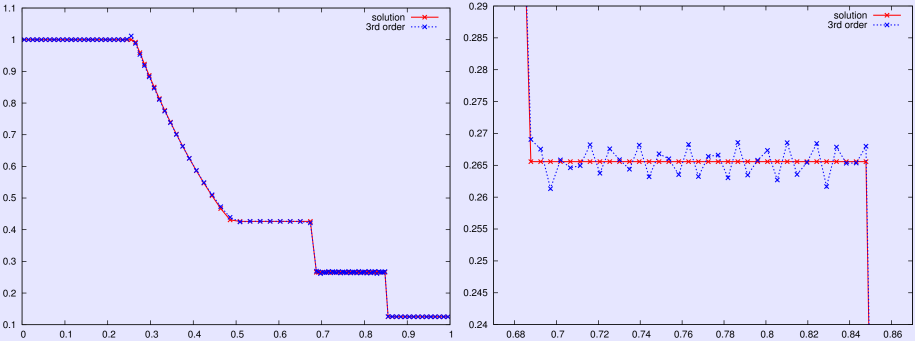

(a) Global view. (b) Zoom on $[0.67, 0.87] \times [0.24, 0.29]$.

FIGURE: Third-order DG scheme solutions for the Sod shock tube problem on 100 cells: density.

Influence of the limitation on the linearized Riemann invariants

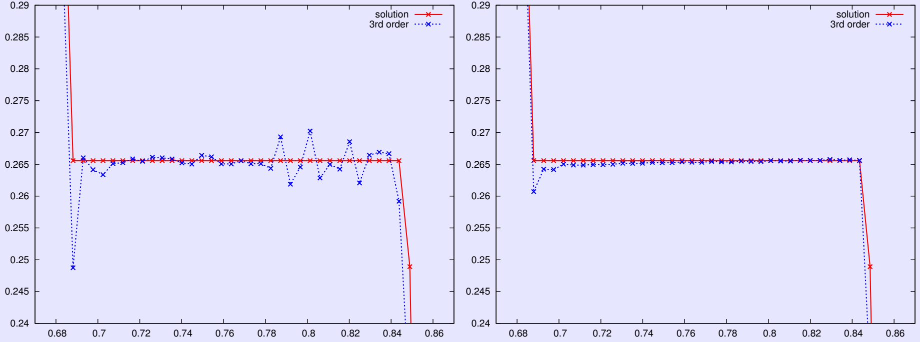

(a) Physical variables limitation.

(b) Riemann invariants limitation.

FIGURE: Third-order DG scheme solutions for the Sod shock tube problem, using 100 cells: density, zoom on $[0.67, 0.87] \times [0.24, 0.29]$.

B. COCKBURN AND C.-W. SHU, *The RKDG method for conservation laws V: Multidimensional systems.* J. Comp. Phys., 1998.

1D Lagrangian gas dynamics

3rd order DG scheme with limitation

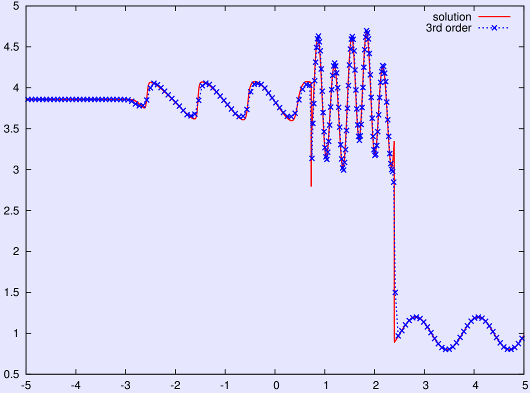

FIGURE: Third-order DG scheme solution with limitation, for a Shu oscillating shock tube problem using 200 cells.

Rate of convergence for the third-order DG scheme

	L_1		L_2		L_∞	
ΔX	E_{L_1}	q_{L_1}	E_{L_2}	q_{L_2}	E_{L_∞}	q_{L_∞}
$\frac{1}{50}$	9.09E-5	3.01	3.40E-4	2.87	2.20E-3	2.79
$\frac{1}{100}$	1.13E-5	3.58	4.64E-5	3.28	3.17E-4	2.70
$\frac{1}{200}$	9.40E-7	3.30	4.79E-6	3.34	4.89E-5	2.64
$\frac{1}{400}$	9.57E-8	3.03	4.74E-7	3.07	7.85E-6	2.91
$\frac{1}{800}$	1.17E-8	-	5.63E-8	-	1.04E-6	-

TABLE: Rate of convergence computed with the particular smooth solution designed in the special case of $\gamma = 3$, on the $[0, 1]$ domain, at time $t = 0.8$ with a CFL$= 0.1$.

F. VILAR, P.-H. MAIRE AND R. ABGRALL, *Cell-centered discontinuous Galerkin discretizations for two-dimensional scalar conservation laws on unstructured grids and for one-dimensional Lagrangian hydrodynamics.* Comp. & Fluids, 2010.

Content

1 Introduction and preliminary results

2 2D Lagrangian hydrodynamics

3 DG discretization general framework

4 Second-order DG scheme

5 Third-order DG scheme

6 Conclusions and perspectives

Cell-Centered Lagrangian schemes

Finite volume schemes on moving mesh

- J. K. Dukowicz: CAVEAT scheme
  A computer code for fluid dynamics problems with large distorsion and internal slip, 1986
- B. Després: GLACE scheme
  Lagrangian Gas Dynamics in Two Dimensions and Lagrangian systems, 2005
- P.-H. Maire: EUCCLHYD scheme
  A cell-centered Lagrangian scheme for two-dimensional compressible flow problems, 2007
- G. Kluth: Hyperelasticity
  Discretization of hyperelasticity with a cell-centered Lagrangian scheme, 2010
- S. Del Pino: Curvilinear Finite Volume method
  A curvilinear finite-volume method to solve compressible gas dynamics in semi-Lagrangian coordinates, 2010
- P. Hoch: Finite Volume method on unstructured conical meshes
  Extension of ALE methodology to unstructured conical meshes, 2011

DG scheme on initial mesh

- R. Loubère: DG scheme for Lagrangian hydrodynamics
  A Lagrangian Discontinuous Galerkin-type method on unstructured meshes to solve hydrodynamics problems, 2004

Lagrangian and Eulerian descriptions

Flow transformation of the fluid

- The fluid flow is described mathematically by the continuous transformation, Φ, so-called mapping such as $\Phi : \boldsymbol{X} \longrightarrow \boldsymbol{x} = \Phi(\boldsymbol{X}, t)$

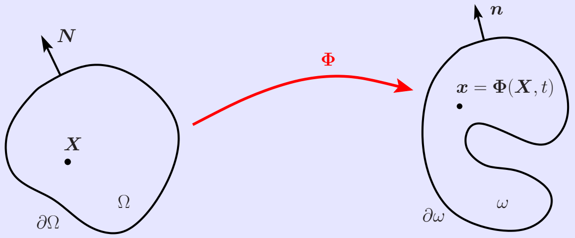

FIGURE: Notation for the flow map.

where $\boldsymbol{X}$ is the Lagrangian (initial) coordinate, $\boldsymbol{x}$ the Eulerian (actual) coordinate, $\boldsymbol{N}$ the Lagrangian normal and $\boldsymbol{n}$ the Eulerian normal

Deformation Jacobian matrix: deformation gradient tensor

- $\mathrm{F} = \nabla_X \Phi = \frac{\partial \boldsymbol{x}}{\partial X}$ and $J = \det \mathrm{F} > 0$

Lagrangian and Eulerian descriptions

Trajectory equation

- $\dfrac{\mathrm{d}\,\boldsymbol{x}}{\mathrm{d}t} = \boldsymbol{U}(\boldsymbol{x}, t), \quad \boldsymbol{x}(\boldsymbol{X}, 0) = \boldsymbol{X}$

Material time derivative

- $\dfrac{\mathrm{d}}{\mathrm{d}t} f(\boldsymbol{x}, t) = \dfrac{\partial}{\partial t} f(\boldsymbol{x}, t) + \boldsymbol{U} \cdot \nabla_x f(\boldsymbol{x}, t)$

Transformation formulas

- $\mathrm{F}\mathrm{d}\boldsymbol{X} = \mathrm{d}\boldsymbol{x}$ — Change of shape of infinitesimal vectors
- $\rho^0 = \rho J$ — Mass conservation
- $J\mathrm{d}V = \mathrm{d}v$ — Measure of the volume change
- $J\mathrm{F}^{-t}\boldsymbol{N}\mathrm{d}S = \boldsymbol{n}\mathrm{d}s$ — **Nanson formula**

Differential operators transformations

- $\boldsymbol{\nabla}_x P = \frac{1}{J}\nabla_X \cdot (P J \mathrm{F}^{-\mathrm{t}})$ — Gradient operator
- $\nabla_x \cdot \boldsymbol{U} = \frac{1}{J}\nabla_X \cdot (J\mathrm{F}^{-1}\boldsymbol{U})$ — Divergence operator

Lagrangian and Eulerian descriptions

Piola compatibility condition

- $\nabla_x \cdot G = \mathbf{0}$, where $\mathrm{G} = J\mathrm{F}^{-t}$ is the cofactor matrix of F

$$\int_{\Omega} \nabla_x \cdot G \, \mathrm{d}V = \int_{\partial\Omega} \mathrm{G}\, \boldsymbol{N} \, \mathrm{d}S = \int_{\partial\omega} \boldsymbol{n} \, \mathrm{d}s = \mathbf{0}$$

Gas dynamics system written in its total Lagrangian form

- $\dfrac{\mathrm{d}\,\mathrm{F}}{\mathrm{d}t} - \nabla_X \boldsymbol{U} = 0$ — Deformation gradient tensor equation
- $\rho^0 \dfrac{\mathrm{d}}{\mathrm{d}t}\left(\dfrac{1}{\rho}\right) - \nabla_X \cdot (\mathrm{G}^t \boldsymbol{U}) = 0$ — Specific volume equation
- $\rho^0 \dfrac{\mathrm{d}\,\boldsymbol{U}}{\mathrm{d}t} + \nabla_X \cdot (P\,\mathrm{G}) = \mathbf{0}$ — Momentum equation
- $\rho^0 \dfrac{\mathrm{d}\,E}{\mathrm{d}t} + \nabla_X \cdot (\mathrm{G}^t P \boldsymbol{U}) = 0$ — Total energy equation

Thermodynamical closure

- EOS: $P = P(\rho, \varepsilon)$ where $\varepsilon = E - \frac{1}{2}\boldsymbol{U}^2$

Content

1 Introduction and preliminary results

2 2D Lagrangian hydrodynamics

3 DG discretization general framework

4 Second-order DG scheme

5 Third-order DG scheme

6 Conclusions and perspectives

DG discretization general framework

$(\alpha+1)^{\text{th}}$ order DG discretization

- Let $\{\Omega_c\}_c$ be a partition of the domain Ω into polygonal cells
- $\{\sigma_k^c\}_{k=0\ldots K}$ basis of $\mathbb{P}^\alpha(\Omega_c)$, where $K+1=\frac{(\alpha+1)(\alpha+2)}{2}$
- $\phi_h^c(\boldsymbol{X},t)=\displaystyle\sum_{k=0}^{K}\phi_k^c(t)\sigma_k^c(\boldsymbol{X})$ approximate function of $\phi(\boldsymbol{X},t)$ on Ω_c

Definitions

- Center of mass $\boldsymbol{\mathcal{X}}_c=(\mathcal{X}_c,\mathcal{Y}_c)^{\text{t}}=\dfrac{1}{m_c}\displaystyle\int_{\Omega_c}\rho^0(\boldsymbol{X})\,\boldsymbol{X}\,\mathrm{d}V$, where m_c is the constant mass of the cell Ω_c
- The mean value $\langle\phi\rangle_c=\dfrac{1}{m_c}\displaystyle\int_{\Omega_c}\rho^0(\boldsymbol{X})\,\phi(\boldsymbol{X})\,\mathrm{d}V$ of the function ϕ over the cell Ω_c
- The associated scalar product $\langle\phi,\psi\rangle_c=\displaystyle\int_{\Omega_c}\rho^0(\boldsymbol{X})\,\phi(\boldsymbol{X})\,\psi(\boldsymbol{X})\,\mathrm{d}V$

Polynomial Taylor basis

Taylor expansion on the cell, located at the center of mass

$$\phi(\boldsymbol{X}) = \phi(\boldsymbol{\mathcal{X}}_c) + \sum_{q=1}^{\alpha}\sum_{j=0}^{q} \frac{(X-\mathcal{X}_c)^{q-j}\,(Y-\mathcal{Y}_c)^j}{j!(q-j)!}\,\frac{\partial^q \phi}{\partial X^{q-j}\partial Y^j}(\boldsymbol{\mathcal{X}}_c) + o(\|\boldsymbol{X}-\boldsymbol{\mathcal{X}}_c\|^{\alpha})$$

$(\alpha+1)^{\text{th}}$ order Polynomial Taylor basis

- The first-order polynomial component and the associated basis function

$$\phi_0^c = \langle \phi \rangle_c \quad \text{and} \quad \sigma_0^c = 1$$

- The q^{th}-order polynomial components and the associated basis functions

$$\phi^c_{\frac{q(q+1)}{2}+j} = (\Delta X_c)^{q-j}(\Delta Y_c)^j\,\frac{\partial^q \phi}{\partial X^{q-j}\partial Y^j}(\boldsymbol{\mathcal{X}}_c),$$

$$\sigma^c_{\frac{q(q+1)}{2}+j} = \frac{1}{j!(q-j)!}\left[\left(\frac{X-\mathcal{X}_c}{\Delta X_c}\right)^{q-j}\left(\frac{Y-\mathcal{Y}_c}{\Delta Y_c}\right)^{j} - \left\langle\left(\frac{X-\mathcal{X}_c}{\Delta X_c}\right)^{q-j}\left(\frac{Y-\mathcal{Y}_c}{\Delta Y_c}\right)^{j}\right\rangle_c\right],$$

where $0 < q \leq \alpha$, $j = 0\ldots q$, $\Delta X_c = \frac{X_{max}-X_{min}}{2}$ and $\Delta Y_c = \frac{Y_{max}-Y_{min}}{2}$

H. Luo, J. D. Baum and R. Löhner, *A DG method based on a Taylor basis for the compressible flows on arbitrary grids.* J. Comp. Phys., 2008.

Polynomial Taylor basis

Outcome

- First moment associated to the basis function $\sigma_0^c = 1$ is the mass averaged value

$$\phi_0^c = \langle \phi \rangle_c$$

- The successive moments can be identified as the successive derivatives of the function expressed at the center of mass of the cell

$$\phi^c_{\frac{q(q+1)}{2}+j} = (\Delta X_c)^{q-j} (\Delta Y_c)^j \, \frac{\partial^q \phi}{\partial X^{q-j} \partial Y^j} (\mathcal{X}_c)$$

- The first basis function is orthogonal to the other ones

$$\langle \sigma_0^c, \sigma_k^c \rangle_c = m_c \, \delta_{0k}$$

- **Same basis functions regardless the shape of the cells** (squares, triangles, generic polygonal cells)

DG discretization general framework

Lagrangian gas dynamics equation type

- $\rho^0 \dfrac{\mathrm{d}\,\phi}{\mathrm{d}t} + \nabla_X \,.\, (\mathrm{G}^{\mathrm{t}} \boldsymbol{f}) = 0$, where $\boldsymbol{f}$ is the flux function

  $\mathrm{G} = J\mathrm{F}^{-\mathrm{t}}$ is the cofactor matrix of F

Local variational formulations

- $$\int_{\Omega_c} \rho^0 \frac{\mathrm{d}\,\phi}{\mathrm{d}t} \sigma_q^c \,\mathrm{d}V = \sum_{k=0}^{K} \frac{\mathrm{d}\,\phi_k^c}{\mathrm{d}t} \int_{\Omega_c} \rho^0 \sigma_q^c \sigma_k^c \,\mathrm{d}V$$
  $$= \int_{\Omega_c} \boldsymbol{f} \,.\, \mathrm{G}\, \boldsymbol{\nabla}_X \sigma_q^c \,\mathrm{d}V - \int_{\partial\Omega_c} \overline{\boldsymbol{f}} \,.\, \sigma_q^c \,\mathrm{G}\boldsymbol{N} \mathrm{d}S$$

Geometric Conservation Law (GCL)

- Equation on the first moment of the specific volume

$$\int_{\Omega_c} \frac{\mathrm{d}\,J}{\mathrm{d}t} \,\mathrm{d}V = \frac{\mathrm{d}\,|\omega_c|}{\mathrm{d}t} = \int_{\Omega_c} \nabla_X \,.\, (\mathrm{G}^{\mathrm{t}} \boldsymbol{U}) \,\mathrm{d}V = \int_{\partial\Omega_c} \overline{\boldsymbol{U}} \,.\, \mathrm{G}\boldsymbol{N} \mathrm{d}S$$

DG discretization general framework

Mass matrix properties

- $\displaystyle\int_{\Omega_c} \rho^0 \sigma_q^c \sigma_k^c \,\mathrm{d}V = \left\langle \sigma_q^c, \sigma_k^c \right\rangle_c$ generic coefficient of the symmetric positive definite mass matrix
- $\left\langle \sigma_0^c, \sigma_k^c \right\rangle_c = m_c \,\delta_{0k}$ mass averaged equation is independent of the other polynomial basis components equations

Interior terms

- $\displaystyle\int_{\Omega_c} \boldsymbol{f} \,.\, \mathrm{G}\, \nabla_X \sigma_q^c \,\mathrm{d}V$ is evaluated through the use of a two-dimensional high-order quadrature rule

Boundary terms

- $\displaystyle\int_{\partial\Omega_c} \overline{\boldsymbol{f}} \,.\, \sigma_q^c \,\mathrm{G}\boldsymbol{N} \mathrm{d}S$ required a specific treatment to ensure the GCL
- It remains to determine the numerical fluxes

Entropic analysis

Entropic semi-discrete equation

- Fundamental assumption $\overline{P\,\boldsymbol{U}} = \overline{P}\,\overline{\boldsymbol{U}}$
- The use of variational formulations and Piola condition leads to

$$\int_{\Omega_c} \rho^0\,\theta \frac{\mathrm{d}\,\eta}{\mathrm{d}t}\,\mathrm{d}V = \int_{\partial\Omega_c} (\overline{P} - P_h)(\boldsymbol{U}_h - \overline{\boldsymbol{U}})\,.\,\mathsf{G}\boldsymbol{N}\mathrm{d}S,$$

where η is the specific entropy and θ the absolute temperature defined by means of the Gibbs identity

Entropic semi-discrete equation

- A sufficient condition to satisfy $\int_{\Omega_c} \rho^0\,\theta \frac{\mathrm{d}\,\eta}{\mathrm{d}t}\,\mathrm{d}V \geq 0$ is

$$\overline{P} - P_h = -Z\,(\overline{\boldsymbol{U}} - \boldsymbol{U}_h)\,.\,\frac{\mathsf{G}\boldsymbol{N}}{\|\mathsf{G}\boldsymbol{N}\|} = -Z\,(\overline{\boldsymbol{U}} - \boldsymbol{U}_h)\,.\,\boldsymbol{n},$$

where $Z \geq 0$ has the physical dimension of a density times a velocity

Riemann invariants limitation

Riemann invariants differentials associated to unit direction $\boldsymbol{n}$

Being given the directions $\boldsymbol{n}$ and $\boldsymbol{t} = \boldsymbol{e}_z \times \boldsymbol{n}$

- $\mathrm{d}\alpha_t = \mathrm{d}\boldsymbol{U} \,.\, \boldsymbol{t}$
- $\mathrm{d}\alpha_- = \mathrm{d}(\frac{1}{\rho}) - \frac{1}{\rho a}\,\mathrm{d}\boldsymbol{U} \,.\, \boldsymbol{n}$
- $\mathrm{d}\alpha_+ = \mathrm{d}(\frac{1}{\rho}) + \frac{1}{\rho a}\,\mathrm{d}\boldsymbol{U} \,.\, \boldsymbol{n}$
- $\mathrm{d}\alpha_E = \mathrm{d}E - \boldsymbol{U} \,.\, \mathrm{d}\boldsymbol{U} + P\,\mathrm{d}(\frac{1}{\rho})$

a denotes the sound speed

Linearization around the mean values in cell Ω_c

- $\alpha^c_{t,h} = \boldsymbol{U}^c_h \,.\, \boldsymbol{t}$
- $\alpha^c_{-,h} = (\frac{1}{\rho})^c_h - \frac{1}{Z_c}\,\boldsymbol{U}^c_h \,.\, \boldsymbol{n}$
- $\alpha^c_{+,h} = (\frac{1}{\rho})^c_h + \frac{1}{Z_c}\,\boldsymbol{U}^c_h \,.\, \boldsymbol{n}$
- $\alpha^c_{E,h} = E^c_h - \boldsymbol{U}^c_0 \,.\, \boldsymbol{U}^c_h + P^c_0\,(\frac{1}{\rho})^c_h$

where $Z_c = a^c_0 \rho^c_0$ is the acoustic impedance

Riemann invariants limitation

System variables polynomial approximation components

- $(\frac{1}{\rho})_k^c = \frac{1}{2}(\alpha_{+,k}^c + \alpha_{-,k}^c)$
- $\boldsymbol{U}_k^c = \frac{1}{2} Z_c(\alpha_{+,k}^c - \alpha_{-,k}^c)\boldsymbol{n} + \alpha_{t,k}^c \boldsymbol{t}$
- $E_k^c = \alpha_{E,k}^c + \frac{1}{2} Z_c(\alpha_{+,k}^c - \alpha_{-,k}^c)\boldsymbol{U}_0^c \cdot \boldsymbol{n} + \alpha_{t,k}^c \boldsymbol{U}_0^c \cdot \boldsymbol{t} - \frac{1}{2} P_0^c(\alpha_{+,k}^c + \alpha_{-,k}^c)$

Unit direction ensuring symmetry preservation

- $\boldsymbol{n} = \dfrac{\boldsymbol{U}_0^c}{\|\boldsymbol{U}_0^c\|}$ and $\boldsymbol{t} = \boldsymbol{e}_z \times \dfrac{\boldsymbol{U}_0^c}{\|\boldsymbol{U}_0^c\|}$

Deformation gradient tensor discretization

Requirements

- **Consistency** of vector $\mathrm{G}\boldsymbol{N}\mathrm{d}S = \boldsymbol{n}\mathrm{d}s$ at the interfaces of the cells
- **Continuity** of vector $\mathrm{G}\boldsymbol{N}$ at cell interfaces on both sides of the interface
- **Preservation of uniform flows**, $\mathrm{G} = J\mathrm{F}^{-t}$ the cofactor matrix

$$\int_{\Omega_c} \mathrm{G}\boldsymbol{\nabla}_X \sigma_q^c \,\mathrm{d}V = \int_{\partial\Omega_c} \sigma_q^c \,\mathrm{G}\boldsymbol{N}\mathrm{d}S \quad \Longleftrightarrow \quad \int_{\Omega_c} \sigma_q^c \left(\nabla_X \cdot \mathrm{G}\right) \mathrm{d}V = \mathbf{0}$$

Generalization of the weak form of the Piola compatibility condition

Tensor F discretization

- Discretization of tensor F by means of a mapping defined on triangular cells
- Partition of the polygonal cells in the initial configuration into non-overlapping triangles

$$\Omega_c = \bigcup_{i=1}^{ntri} \mathcal{T}_i^c$$

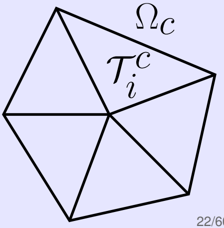

Deformation gradient tensor discretization

Continuous mapping function

- We develop Φ on the Finite Elements basis functions λ_p

$$\Phi_h^i(\boldsymbol{X}, t) = \sum_p \lambda_p(\boldsymbol{X})\ \Phi_p(t),$$

where the points p are control points including vertices in $\mathcal{T}_i$

- $\Phi_p(t) = \Phi(\boldsymbol{X}_p, t) = \boldsymbol{x}_p$
- $\dfrac{\mathrm{d}\,\Phi_p}{\mathrm{d}t} = \boldsymbol{U}_p \Longrightarrow \dfrac{\mathrm{d}}{\mathrm{d}t}\mathsf{F}_i(\boldsymbol{X}, t) = \sum_p \boldsymbol{U}_p(t) \otimes \nabla_X \lambda_p(\boldsymbol{X})$

G. Kluth and B. Després, *Discretization of hyperelasticity on unstructured mesh with a cell-centered Lagrangian scheme.* J. Comp. Phys., 2010.

Outcome

- Satisfaction of the Piola compatibility condition **everywhere**
- **Consistency** and **continuity** of the Eulerian normal G$\boldsymbol{N}$

Content

1 Introduction and preliminary results

2 2D Lagrangian hydrodynamics

3 DG discretization general framework

4 Second-order DG scheme

5 Third-order DG scheme

6 Conclusions and perspectives

Geometry discretization

P_1 barycentric coordinate basis functions

- In a generic triangle $\mathcal{T}_i$

$$\lambda_p(\boldsymbol{X}) = \frac{1}{2|\mathcal{T}_i|}[X(Y_{p^+} - Y_{p^-}) - Y(X_{p^+} - X_{p^-}) + X_{p^+}Y_{p^-} - X_{p^-}Y_{p^+}],$$

where p, p^+ and p^- are the counterclockwise ordered triangle nodes and $|\mathcal{T}_i|$ the triangle volume

Deformation gradient tensor discretization

- $\Phi_h^i(\boldsymbol{X}, t) = \sum_{p \in \mathcal{P}(\mathcal{T}_i)} \lambda_p(\boldsymbol{X})\, \boldsymbol{x}_p(t),$

where $\mathcal{P}(\mathcal{T}_i)$ is the node set of $\mathcal{T}_i$

- $\frac{\mathrm{d}}{\mathrm{d}t}\mathsf{F}_i(t) = \frac{1}{|\mathcal{T}_i|} \sum_{p \in \mathcal{P}(\mathcal{T}_i)} \boldsymbol{U}_p(t) \otimes L_{pi}\boldsymbol{N}_{pi}$

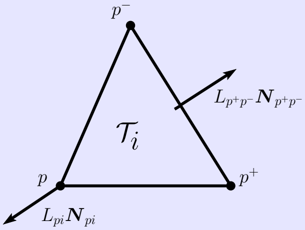

Local variational formulations

DG discretization of the Lagrangian gas dynamics equations type

- $\mathsf{G}_i^c = (\mathsf{J}\mathsf{F}^{-t})_i^c$ is constant on $\mathcal{T}_i^c$ and $\nabla_{\boldsymbol{X}} \sigma_q$ constant over Ω_c
- $\displaystyle\int_{\Omega_c} \rho^0 \frac{\mathrm{d}\,\phi}{\mathrm{d}t} \sigma_q^c \,\mathrm{d}V = -\sum_{i=1}^{ntri} \mathsf{G}_i^c \nabla_X \sigma_q^c \,\boldsymbol{.} \int_{\mathcal{T}_i^c} \boldsymbol{f} \,\mathrm{d}V + \sum_{p\in\mathcal{P}(c)} \int_p^{p^+} \overline{\boldsymbol{f}} \,\boldsymbol{.}\, \sigma_q^c \,\mathsf{G}\boldsymbol{N} \mathrm{d}L$

Linear assumptions on face f_{pp^+}

- $\overline{\boldsymbol{f}}^{\,c}_{|_{pp^+}}(\zeta) = \boldsymbol{f}_{pc}^{+}\,(1-\zeta) + \boldsymbol{f}_{p^+c}^{-}\,\zeta,$

  where $\boldsymbol{f}_{pc}^{+}$ and $\boldsymbol{f}_{p^+c}^{-}$ are respectively the right and left nodal numerical fluxes

Linear property on face f_{pp^+}

- $\sigma^c_{q|_{pp^+}}(\zeta) = \sigma_q^c(\boldsymbol{X}_p)\,(1-\zeta) + \sigma_q^c(\boldsymbol{X}_{p^+})\,\zeta,$

  where $\sigma_q^c(\boldsymbol{X}_p)$ and $\sigma_q^c(\boldsymbol{X}_{p^+})$ are the extrapolated values of the function σ_q^c

Initial configuration cell

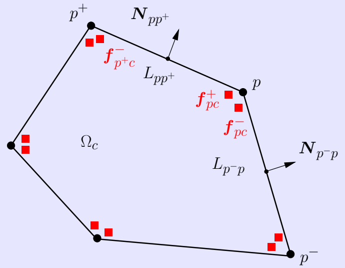

DG discretization

Fundamental assumptions

- $\boldsymbol{U}_{pc}^{\pm} = \boldsymbol{U}_p, \quad \forall c \in \mathcal{C}(p)$
- $\overline{P\boldsymbol{U}} = \overline{P}\,\overline{\boldsymbol{U}} \quad \Longrightarrow \quad (P\boldsymbol{U})_{pc}^{\pm} = P_{pc}^{\pm}\,\boldsymbol{U}_p$

Procedure

- Analytical integration + index permutation

Weighted corner normals

- $l_{pc}^{q}\boldsymbol{n}_{pc}^{q} = l_{pc}^{-,q}\boldsymbol{n}_{pc}^{-,q} + l_{pc}^{+,q}\boldsymbol{n}_{pc}^{+,q}$
- $l_{pc}^{+,q}\boldsymbol{n}_{pc}^{+,q} = \dfrac{1}{6}\left(2\sigma_q^c(\boldsymbol{X}_p) + \sigma_q^c(\boldsymbol{X}_{p^+})\right)\, l_{pp^+}\boldsymbol{n}_{pp^+}$
- $l_{pc}^{-,q}\boldsymbol{n}_{pc}^{-,q} = \dfrac{1}{6}\left(2\sigma_q^c(\boldsymbol{X}_p) + \sigma_q^c(\boldsymbol{X}_{p^-})\right)\, l_{p^-p}\boldsymbol{n}_{p^-p}$

q^{th} moment of the subcell forces

- $\boldsymbol{F}_{pc}^{q} = P_{pc}^{-}\, l_{pc}^{-,q}\boldsymbol{n}_{pc}^{-,q} + P_{pc}^{+}\, l_{pc}^{+,q}\boldsymbol{n}_{pc}^{+,q}$

Local variational formulations

Semi-discrete equations GCL compatible

- $$\int_{\Omega_c} \rho^0 \frac{\mathrm{d}}{\mathrm{d}t}\left(\frac{1}{\rho}\right)\sigma_q^c \,\mathrm{d}V = -\sum_{i=1}^{ntri} \mathrm{G}_i^c \nabla_X \sigma_q^c \,.\, \int_{\mathcal{T}_i^c} \boldsymbol{U} \mathrm{d}V + \sum_{p\in\mathcal{P}(c)} \boldsymbol{U}_p \,.\, l_{pc}^q \boldsymbol{n}_{pc}^q$$
- $$\int_{\Omega_c} \rho^0 \frac{\mathrm{d}\,\boldsymbol{U}}{\mathrm{d}t}\sigma_q^c \,\mathrm{d}V = \sum_{i=1}^{ntri} \mathrm{G}_i^c \nabla_X \sigma_q^c \int_{\mathcal{T}_i^c} P \mathrm{d}V - \sum_{p\in\mathcal{P}(c)} \boldsymbol{F}_{pc}^q$$
- $$\int_{\Omega_c} \rho^0 \frac{\mathrm{d}\,E}{\mathrm{d}t}\sigma_q^c \,\mathrm{d}V = \sum_{i=1}^{ntri} \mathrm{G}_i^c \nabla_X \sigma_q^c \,.\, \int_{\mathcal{T}_i^c} P\,\boldsymbol{U} \mathrm{d}V - \sum_{p\in\mathcal{P}(c)} \boldsymbol{U}_p \,.\, \boldsymbol{F}_{pc}^q$$

First moment equations

- $$m_c \frac{\mathrm{d}}{\mathrm{d}t}\left(\frac{1}{\rho}\right)_0^c = \sum_{p\in\mathcal{P}(c)} \boldsymbol{U}_p \,.\, l_{pc}^0 \boldsymbol{n}_{pc}^0$$
- $$m_c \frac{\mathrm{d}\,E_0^c}{\mathrm{d}t} = -\sum_{p\in\mathcal{P}(c)} \boldsymbol{U}_p \,.\, \boldsymbol{F}_{pc}^0$$
- $$m_c \frac{\mathrm{d}\,\boldsymbol{U}_0^c}{\mathrm{d}t} = -\sum_{p\in\mathcal{P}(c)} \boldsymbol{F}_{pc}^0$$

We recover the EUCCLHYD scheme

Nodal solvers

q^{th} moment of the subcell forces

- The use of $\overline{P} = P_h^c - Z_c\,(\overline{\boldsymbol{U}} - \boldsymbol{U}_h^c)\,.\,\boldsymbol{n}$ to calculate $\boldsymbol{F}_{pc}^q$ leads to

$$\boldsymbol{F}_{pc}^q = P_h^c(\boldsymbol{X}_p, t)\, l_{pc}^q \boldsymbol{n}_{pc}^q - \mathsf{M}_{pc}^q\,(\boldsymbol{U}_p - \boldsymbol{U}_h^c(\boldsymbol{X}_p, t)),$$

where $\mathsf{M}_{pc}^q = Z_c \left(l_{pc}^{-,q} \boldsymbol{n}_{pc}^{-,q} \otimes \boldsymbol{n}_{pc}^{-,0} + l_{pc}^{+,q} \boldsymbol{n}_{pc}^{+,q} \otimes \boldsymbol{n}_{pc}^{+,0} \right)$

Momentum and total energy conservation

- $\displaystyle\sum_{c \in \mathcal{C}(p)} \boldsymbol{F}_{pc}^0 = \boldsymbol{0}$

Nodal velocity

- $\displaystyle\Big(\sum_{c \in \mathcal{C}(p)} M_{pc}^0 \Big)\, \boldsymbol{U}_p = \sum_{c \in \mathcal{C}(p)} \left[P_h^c(\boldsymbol{X}_p, t)\, l_{pc}^0 \boldsymbol{n}_{pc}^0 + \mathsf{M}_{pc}^0\, \boldsymbol{U}_h^c(\boldsymbol{X}_p, t) \right]$

Sedov point blast problem on a Cartesian grid

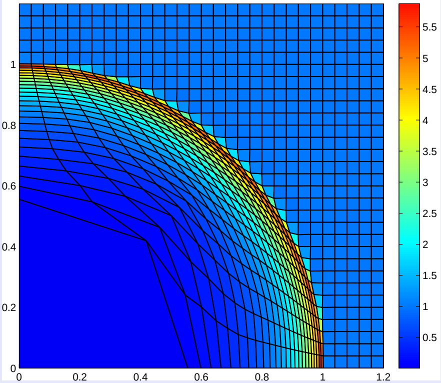

(a) Second-order scheme.

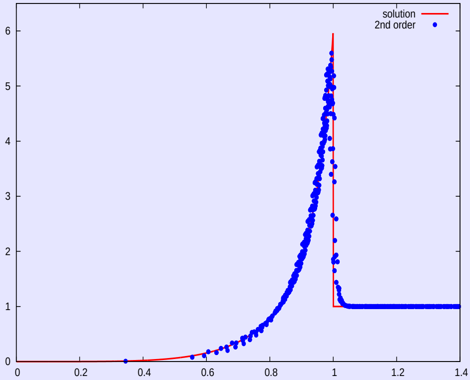

(b) Density profile.

FIGURE: Point blast Sedov problem on a Cartesian grid made of 30 $\times$ 30 cells: density.

Sedov point blast problem on unstructured grids

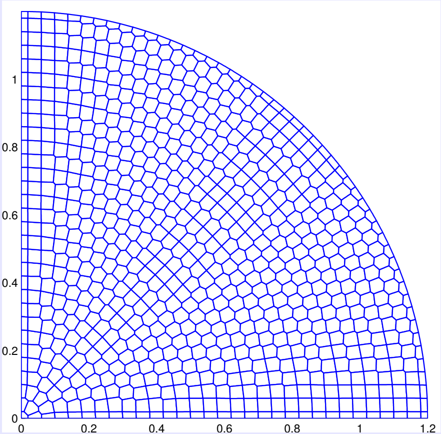

(a) Polygonal grid.

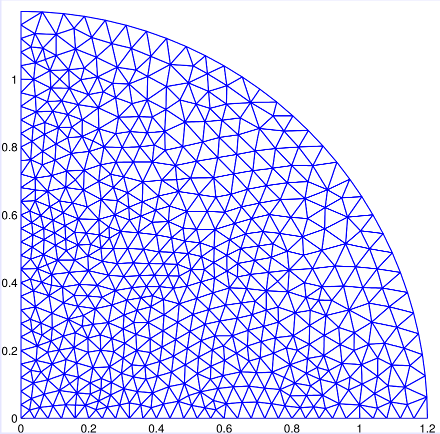

(b) Triangular grid.

FIGURE: Unstructured initial grids for the point blast Sedov problem.

Sedov point blast problem a polygonal grid

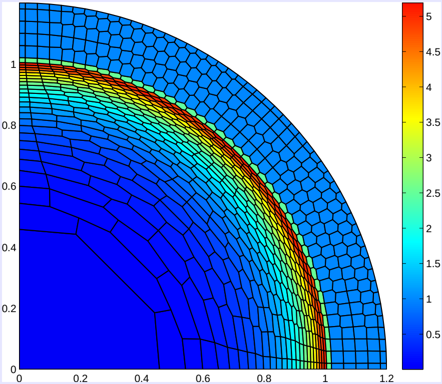

(a) Second-order scheme.

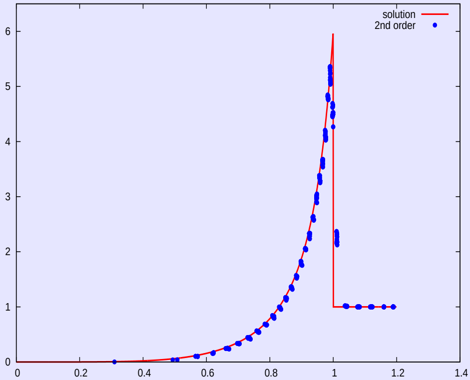

(b) Density profile.

FIGURE: Point blast Sedov problem on an unstructured grid made of 775 polygonal cells: density map.

Sedov point blast problem on a triangular grid

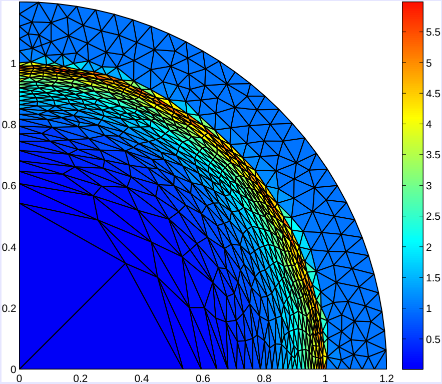

(a) Second-order scheme.

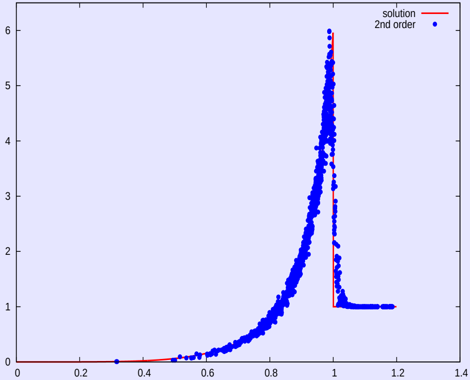

(b) Density profile.

FIGURE: Point blast Sedov problem on an unstructured grid made of 1100 triangular cells: density map.

Noh problem

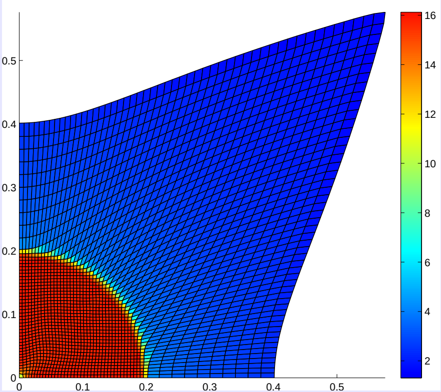

(a) Second-order scheme.

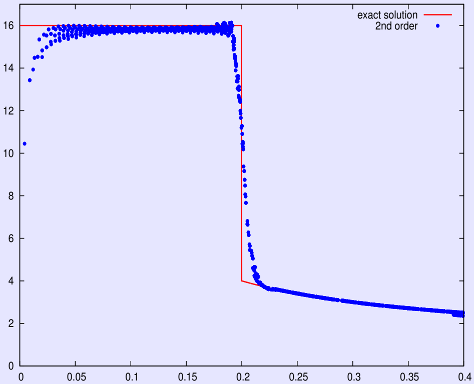

(b) Density profile.

FIGURE: Noh problem on a Cartesian grid made of 50 $\times$ 50 cells: density.

Numerical results

Taylor-Green vortex problem, introduced by R. Rieben (LLNL)

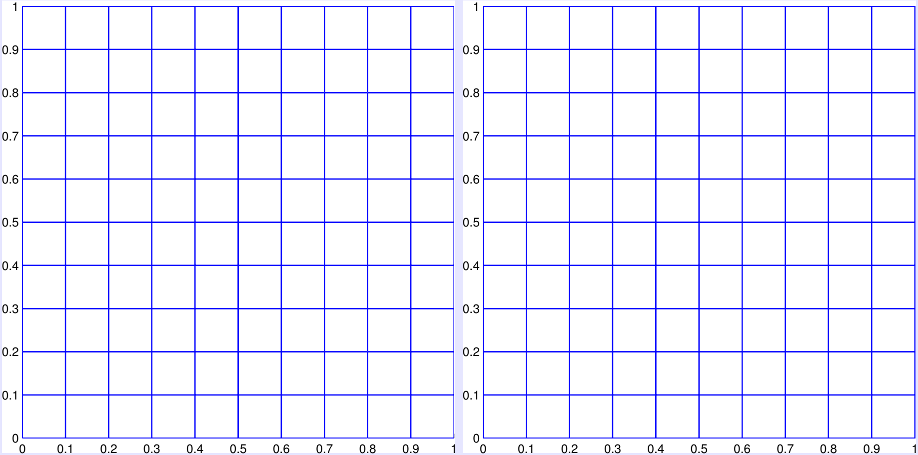

(a) Second-order scheme. (b) Exact solution.

FIGURE: Motion of a 10×10 Cartesian mesh through a T.-G. vortex, at $t = 0.75$.

Rate of convergence computed on the pressure in the case of the Taylor-Green vortex

	L_1		L_2		L_∞	
h	$E^h_{L_1}$	$q^h_{L_1}$	$E^h_{L_2}$	$q^h_{L_2}$	$E^h_{L_\infty}$	$q^h_{L_\infty}$
$\frac{1}{20}$	1.32E-2	1.78	1.96E-2	1.56	7.41E-2	1.03
$\frac{1}{40}$	3.84E-3	1.93	6.66E-3	1.89	3.63E-2	1.58
$\frac{1}{80}$	1.01E-3	1.99	1.80E-3	1.98	1.21E-2	1.87
$\frac{1}{160}$	2.55E-4	2.00	4.57E-4	2.00	3.31E-3	1.97
$\frac{1}{320}$	6.38E-5	-	1.14E-4	-	8.47E-4	-

TABLE: Second-order MUSCL scheme without limitation at time $t = 0.6$.

	L_1		L_2		L_∞	
h	$E^h_{L_1}$	$q^h_{L_1}$	$E^h_{L_2}$	$q^h_{L_2}$	$E^h_{L_\infty}$	$q^h_{L_\infty}$
$\frac{1}{20}$	8.98E-3	1.88	1.51E-2	1.75	6.73E-2	1.27
$\frac{1}{40}$	2.44E-3	1.94	4.48E-3	1.95	2.79E-2	1.68
$\frac{1}{80}$	6.36E-4	2.00	1.16E-3	2.00	8.68E-3	1.95
$\frac{1}{160}$	1.59E-4	2.01	2.90E-4	2.01	2.24E-3	2.01
$\frac{1}{320}$	3.94E-5	-	7.18E-5	-	5.54E-4	-

TABLE: Second-order DG scheme without limitation at time $t = 0.6$.

Content

1 Introduction and preliminary results

2 2D Lagrangian hydrodynamics

3 DG discretization general framework

4 Second-order DG scheme

5 Third-order DG scheme

6 Conclusions and perspectives

Curvilinear elements motivation

Circular polar grid: 10 × 1 cells

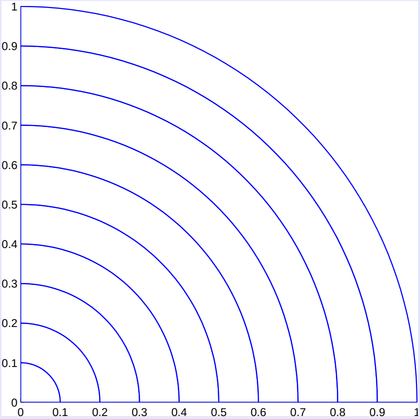

Taylor-Green exact motion

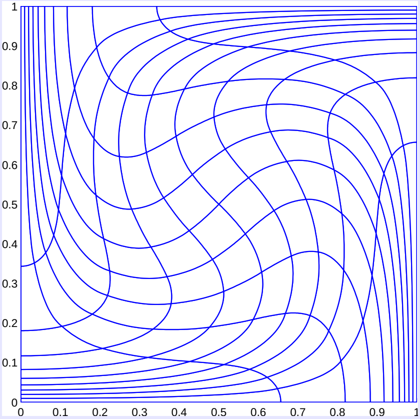

V. DOBREV, T. ELLIS, T. KOLEV AND R. RIEBEN, *High Order Curvilinear Finite Elements for Lagrangian Hydrodynamics. Part I: General Framework*, 2010. Presentation available at https://computation.llnl.gov/casc/blast/blast.html

Geometry discretization

P_2 Finite Elements basis functions

- The P_2 barycentric coordinate functions μ_p write

$$\mu_p = (\lambda_p)^2,\ \mu_{p^+} = (\lambda_{p^+})^2,\ \mu_{p^-} = (\lambda_{p^-})^2,$$
$$\mu_Q = 2\lambda_p\lambda_{p^+},\ \mu_{Q^+} = 2\lambda_{p^+}\lambda_{p^-},\ \mu_{Q^-} = 2\lambda_{p^-}\lambda_p,$$

where $\{\lambda_l\}_{l\in\mathcal{P}(\mathcal{T}_i)}$ is the P_1 Finite Elements linear basis

Mapping discretization

$$\Phi(\boldsymbol{X},t) = \sum_q \boldsymbol{x}_q(t)\,\mu_q(\boldsymbol{X}) = \sum_{p\in\mathcal{P}(\mathcal{T}_i)} \left[\boldsymbol{x}_p(t)\,(\lambda_p(\boldsymbol{X}))^2 + 2\boldsymbol{x}_Q(t)\,\lambda_p(\boldsymbol{X})\lambda_p^+(\boldsymbol{X})\right]$$

Deformation gradient tensor discretization

$$\frac{\mathrm{d}}{\mathrm{d}t}\mathsf{F}_i(\boldsymbol{X},t) = \frac{2}{|\mathcal{T}_i|}\sum_{p\in\mathcal{P}(\mathcal{T}_i)} \lambda_p(\boldsymbol{X})\left[\boldsymbol{U}_p\otimes L_{pc}\boldsymbol{N}_{pc} + \boldsymbol{U}_Q\otimes L_{p^+c}\boldsymbol{N}_{p^+c} + \boldsymbol{U}_Q^-\otimes L_{p^-c}\boldsymbol{N}_{p^-c}\right]$$

Geometric consideration

Mapping of the fluid flow: transformation of $\mathcal{T}_i$ into τ_i

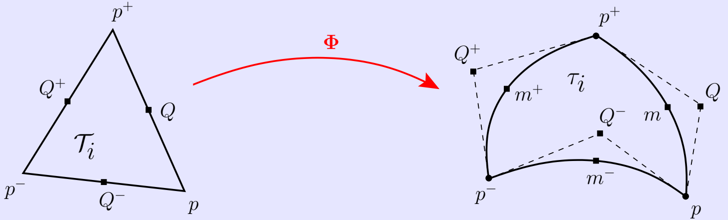

Bezier curves

- Given the three points p, Q and p^+, and $\zeta \in [0, 1]$

$$\begin{aligned} \boldsymbol{x}(\zeta) &= (1-\zeta)^2 \boldsymbol{x}_p + 2\zeta(1-\zeta)\boldsymbol{x}_Q + \zeta^2 \boldsymbol{x}_{p^+} \\ &= (1-\zeta)(1-2\zeta)\boldsymbol{x}_p + 4\zeta(1-\zeta)\boldsymbol{x}_m + \zeta(2\zeta-1)\boldsymbol{x}_{p^+} \end{aligned}$$

- Midpoint $\quad \boldsymbol{x}_m = \boldsymbol{x}(\tfrac{1}{2}) = \dfrac{2\boldsymbol{x}_Q + \boldsymbol{x}_p + \boldsymbol{x}_{p^+}}{4}$

- Tangent $\quad \boldsymbol{t}\,\mathrm{d}l = \dfrac{\mathrm{d}\boldsymbol{x}}{\mathrm{d}\zeta}\,\mathrm{d}\zeta = 2\left((1-\zeta)(\boldsymbol{x}_Q - \boldsymbol{x}_p) + \zeta(\boldsymbol{x}_{p^+} - \boldsymbol{x}_Q)\right)\mathrm{d}\zeta$

DG discretization

Local variational formulations

- $$\int_{\Omega_c} \rho^0 \frac{\mathrm{d}\,\phi}{\mathrm{d}t} \sigma_q^c \,\mathrm{d}V = -\sum_{i=1}^{ntri} \int_{\mathcal{T}_i^c} \mathsf{G}\, \nabla_X \sigma_q^c \,.\, \boldsymbol{f} \,\mathrm{d}V + \sum_{p \in \mathcal{P}(c)} \int_p^{p^+} \overline{\boldsymbol{f}} \,.\, \sigma_q^c \,\mathsf{G}\boldsymbol{N}\mathrm{d}L$$

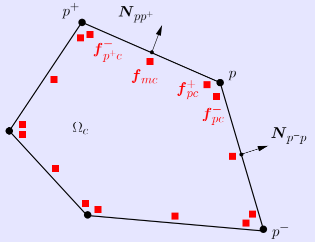

Quadratic assumptions on face f_{pp^+}

- $\boldsymbol{f}_{|_{pp^+}}(\zeta) = (1-\zeta)(1-2\zeta)\,\boldsymbol{f}^+_{pc} + 4\zeta(1-\zeta)\,\boldsymbol{f}_{mc} + \zeta(2\zeta-1)\,\boldsymbol{f}^-_{p^+c}$

Linear and quadratic properties on face f_{pp^+}

- $\mathsf{G}\,\boldsymbol{N}\,\mathrm{d}L_{|_{pp^+}}(\zeta) = 2\left((1-\zeta)\, l_{pQ}\boldsymbol{n}_{pQ} + \zeta\, l_{Qp^+}\boldsymbol{n}_{Qp^+}\right)\mathrm{d}\zeta$
- $\sigma^c_{q|_{pp^+}}(\zeta) = (1-\zeta)(1-2\zeta)\,\sigma_q^c(\boldsymbol{X}_p) + 4\zeta(1-\zeta)\,\sigma_q^c(\boldsymbol{X}_m) + \zeta(2\zeta-1)\,\sigma_q^c(\boldsymbol{X}_{p^+})$

DG discretization

Semi-discrete equations GCL compatible

$$\int_{\Omega_c} \rho^0 \frac{\mathrm{d}}{\mathrm{d}t}\left(\frac{1}{\rho}\right)\sigma_q^c \,\mathrm{d}V = -\sum_{i=1}^{ntri} \int_{\mathcal{T}_i^c} \boldsymbol{U}\,.\,\mathrm{G}\nabla_X \sigma_q^c \mathrm{d}V + \sum_{p\in\mathcal{P}(c)} \frac{1}{3}\boldsymbol{U}_p\,.\,l_{pc}^q \boldsymbol{n}_{pc}^q + \sum_{m\in\mathcal{M}(c)} \frac{2}{3}\boldsymbol{U}_m\,.\,l_{mc}^q \boldsymbol{n}_{mc}^q$$

$$\int_{\Omega_c} \rho^0 \frac{\mathrm{d}\,\boldsymbol{U}}{\mathrm{d}t}\sigma_q^c \,\mathrm{d}V = \sum_{i=1}^{ntri} \int_{\mathcal{T}_i^c} P\mathrm{G}\nabla_X \sigma_q^c \mathrm{d}V - \sum_{p\in\mathcal{P}(c)} \frac{1}{3}\boldsymbol{F}_{pc}^q - \sum_{m\in\mathcal{M}(c)} \frac{2}{3}\boldsymbol{F}_{mc}^q$$

$$\int_{\Omega_c} \rho^0 \frac{\mathrm{d}\,E}{\mathrm{d}t}\sigma_q^c \,\mathrm{d}V = -\sum_{i=1}^{ntri} \int_{\mathcal{T}_i^c} P\boldsymbol{U}\,.\,\mathrm{G}\nabla_X \sigma_q^c \mathrm{d}V + \sum_{p\in\mathcal{P}(c)} \frac{1}{3}\boldsymbol{U}_p\,.\,\boldsymbol{F}_{pc}^q + \sum_{m\in\mathcal{M}(c)} \frac{2}{3}\boldsymbol{U}_m\,.\,\boldsymbol{F}_{mc}^q$$

Equation on the first moment of the specific volume

- $$\frac{\mathrm{d}\,|\omega_c|}{\mathrm{d}t} = \int_{\partial\Omega_c} \overline{\boldsymbol{U}}\,.\,\mathrm{G}\boldsymbol{N}\mathrm{d}L = \sum_{p\in\mathcal{P}(c)} \frac{1}{3}\boldsymbol{U}_p\,.\,l_{Q^-Q}\boldsymbol{n}_{Q^-Q} + \sum_{m\in\mathcal{M}(c)} \frac{2}{3}\boldsymbol{U}_m\,.\,l_{pp^+}\boldsymbol{n}_{pp^+}$$

B. BOUTIN, E. DERIAZ, P. HOCH, P. NAVARO, *Extension of ALE methodology to unstructured conical meshes*, ESAIM: Proceedings, 2011

Nodal and midpoint solvers

Subcell forces definitions

- $\boldsymbol{F}_{pc}^{q} = P_{pc}^{-}\, l_{pc}^{-,q}\boldsymbol{n}_{pc}^{-,q} + P_{pc}^{+}\, l_{pc}^{+,q}\boldsymbol{n}_{pc}^{+,q}$ and $\boldsymbol{F}_{mc}^{q} = P_{mc}\, l_{mc}^{q}\boldsymbol{n}_{pc}^{q}$

q^{th} moment of the nodal and midpoint subcell forces

- The use of $\overline{P} = P_h^c - Z_c\,(\overline{\boldsymbol{U}} - \boldsymbol{U}_h^c)\,.\,\boldsymbol{n}$ to calculate $\boldsymbol{F}_{pc}^{q}$ and $\boldsymbol{F}_{mc}^{q}$ leads to

$$\boldsymbol{F}_{pc}^{q} = P_h^c(\boldsymbol{X}_p, t)\, l_{pc}^{q}\boldsymbol{n}_{pc}^{q} - \mathrm{M}_{pc}^{q}\,(\boldsymbol{U}_p - \boldsymbol{U}_h^c(\boldsymbol{X}_p, t)),$$

$$\boldsymbol{F}_{mc}^{q} = P_h^c(\boldsymbol{X}_m, t)\, l_{mc}^{q}\boldsymbol{n}_{mc}^{q} - \mathrm{M}_{mc}^{q}\,(\boldsymbol{U}_m - \boldsymbol{U}_h^c(\boldsymbol{X}_m, t)),$$

$\mathrm{M}_{pc}^{q} = Z_c\,\left(l_{pc}^{-,q}\boldsymbol{n}_{pc}^{-,q} \otimes \boldsymbol{n}_{pc}^{-,0} + l_{pc}^{+,q}\boldsymbol{n}_{pc}^{+,q} \otimes \boldsymbol{n}_{pc}^{+,0}\right)$ and $\mathrm{M}_{mc}^{q} = Z_c\, l_{mc}^{q}\boldsymbol{n}_{mc}^{q} \otimes \boldsymbol{n}_{mc}^{0}$

Momentum and total energy conservation

- $\sum_{c \in \mathcal{C}(p)} \boldsymbol{F}_{pc}^{0} = \boldsymbol{0}$ and $\boldsymbol{F}_{mL}^{0} + \boldsymbol{F}_{mR}^{0} = \boldsymbol{0}$

Nodal and midpoint solvers

Nodal velocity

- $M_p \boldsymbol{U}_p = \sum_{c \in \mathcal{C}(p)} \left[P_h^c(\boldsymbol{X}_p, t)\, l_{pc}^0 \boldsymbol{n}_{pc}^0 + \mathrm{M}_{pc}^0\, \boldsymbol{U}_h^c(\boldsymbol{X}_p, t) \right],$

  where $\mathrm{M_p} = \sum_{c \in \mathcal{C}(p)} \mathrm{M}_{pc}^0$ is a **positive definite** matrix

Midpoint velocity

- $\mathrm{M}_m\, \boldsymbol{U}_m = \mathrm{M}_m \left(\frac{Z_L\, \boldsymbol{U}_h^L(\boldsymbol{X}_m) + Z_R\, \boldsymbol{U}_h^R(\boldsymbol{X}_m)}{Z_L + Z_R} \right) - \frac{P_h^R(\boldsymbol{X}_m) - P_h^L(\boldsymbol{X}_m)}{Z_L + Z_R}\, l_{mc}^0 \boldsymbol{n}_{mc}^0,$

  where $\mathrm{M}_m = \frac{1}{Z_L}\mathrm{M}_{mL}^0 = \frac{1}{Z_R}\mathrm{M}_{mR}^0 = l_{mc}^0 \boldsymbol{n}_{mc}^0 \otimes \boldsymbol{n}_{mc}^0$ is **positive semi-definite**

1D approximate Riemann problem solution

- $(\boldsymbol{U}_m \,.\, \boldsymbol{n}_{mc}^0) = \left(\frac{Z_L\, \boldsymbol{U}_h^L(\boldsymbol{X}_m) + Z_R\, \boldsymbol{U}_h^R(\boldsymbol{X}_m)}{Z_L + Z_R} \right) .\, \boldsymbol{n}_{mc}^0 - \frac{P_h^R(\boldsymbol{X}_m) - P_h^L(\boldsymbol{X}_m)}{Z_L + Z_R}$

Nodal and midpoint solvers

Tangential component of the midpoint velocity

- $(\boldsymbol{U}_m \cdot \boldsymbol{t}^0_{mc}) = \left(\dfrac{Z_L\, \boldsymbol{U}^L_h(\boldsymbol{X}_m) + Z_R\, \boldsymbol{U}^R_h(\boldsymbol{X}_m)}{Z_L + Z_R} \right) \cdot \boldsymbol{t}^0_{mc}$

Midpoint velocity

- $\boldsymbol{U}_m = \dfrac{Z_L\, \boldsymbol{U}^L_h(\boldsymbol{X}_m) + Z_R\, \boldsymbol{U}^R_h(\boldsymbol{X}_m)}{Z_L + Z_R} - \dfrac{P^R_h(\boldsymbol{X}_m) - P^L_h(\boldsymbol{X}_m)}{Z_L + Z_R}\, \boldsymbol{n}^0_{mc}$

Control point velocity

- $\boldsymbol{U}_Q = \dfrac{4\boldsymbol{U}_m - \boldsymbol{U}_p - \boldsymbol{U}_{p^+}}{2}$

Interior points velocity

- $\boldsymbol{U}_i = \boldsymbol{U}^c_h(\boldsymbol{X}_i, t)$

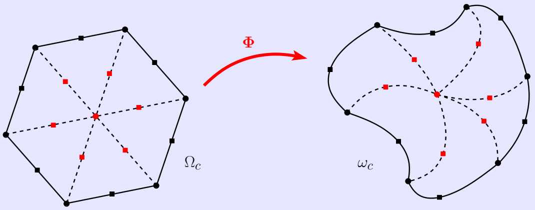

Deformed initial mesh

Composed derivatives

- $$\begin{aligned} \mathrm{F}_T &= \nabla_{X_r} \boldsymbol{\Phi}_T(\boldsymbol{X}_r, t) \\ &= \nabla_X \boldsymbol{\Phi}_H(\boldsymbol{X}, t) \circ \nabla_{X_r} \boldsymbol{\Phi}_0(\boldsymbol{X}_r) \\ &= \mathrm{F}_H\,\mathrm{F}_0 \end{aligned}$$
- $J_T(\boldsymbol{X}_r, t) = J_H(\boldsymbol{X}, t)\, J_0(\boldsymbol{X}_r)$

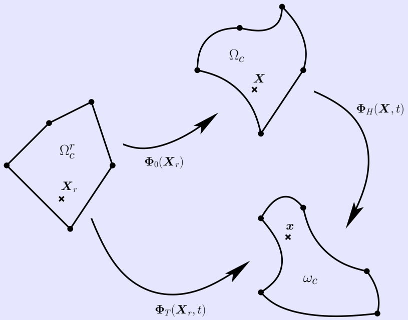

Mass conservation

- $\rho^0\, J_0 = \rho\, J_T$

Modification of the mass matrix

- $\displaystyle\int_{\omega_c} \rho \frac{\mathrm{d}\,\psi_h^c}{\mathrm{d}t} \sigma_q \,\mathrm{d}\omega = \sum_{k=0}^{K} \frac{\mathrm{d}\,\psi_k}{\mathrm{d}t} \int_{\Omega_c^r} \rho^0\, J_0\, \sigma_q\, \sigma_k \,\mathrm{d}\Omega^r$ time rate of change of successive moments of function ψ
- New definitions of mass matrix, of mass averaged value and of the associated scalar product

One angular cell polar Sod shock tube problem

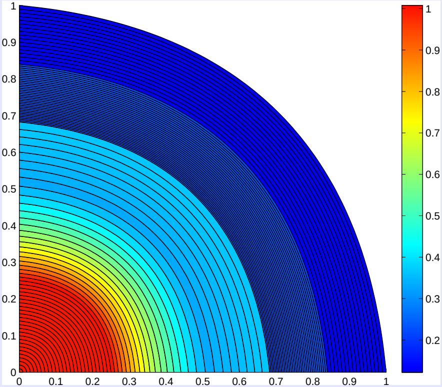

(a) Density map.

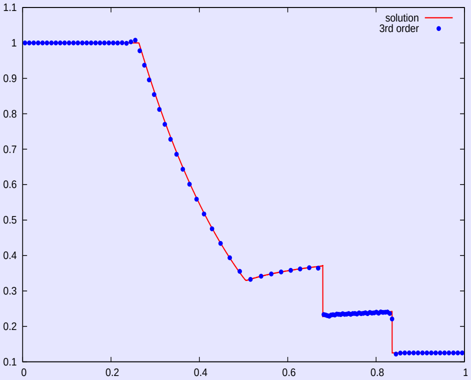

(b) Density profile.

FIGURE: Third-order DG solution for a Sod shock tube problem on a polar grid made of 100×1 cells.

Symmetry preservation

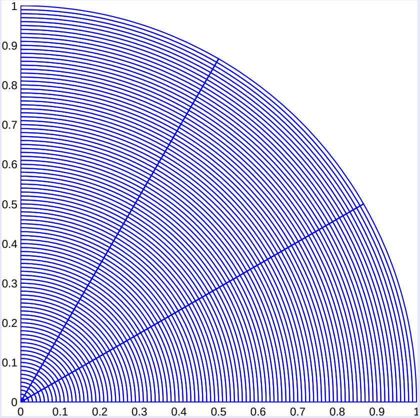

(a) Uniform grid.

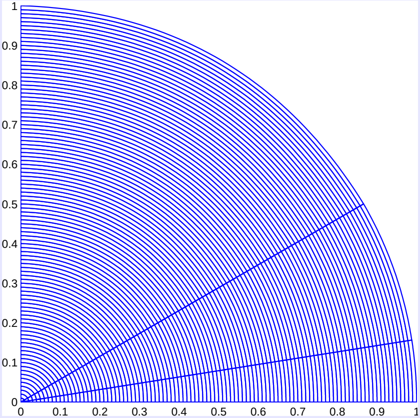

(b) Non-uniform grid.

FIGURE: Polar initial grids for the Sod shock tube problem.

Symmetry preservation

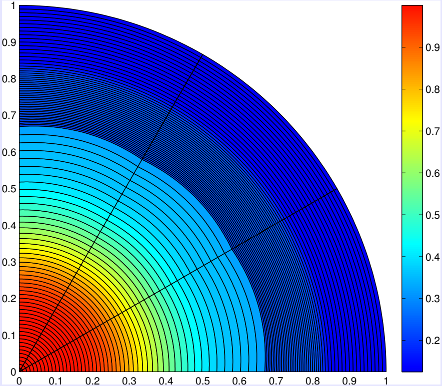

(a) First-order scheme.

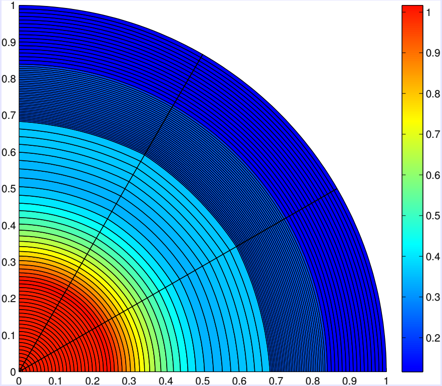

(b) Second-order scheme.

FIGURE: Sod shock tube problem on a polar grid made of 100 $\times$ 3 cells.

Symmetry preservation

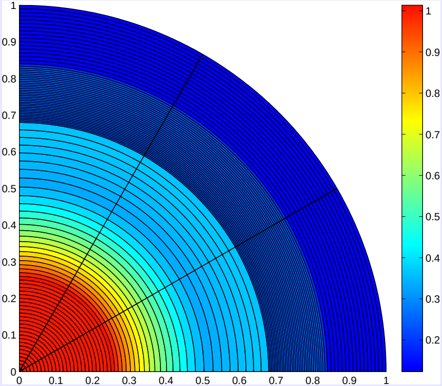

(a) Density map.

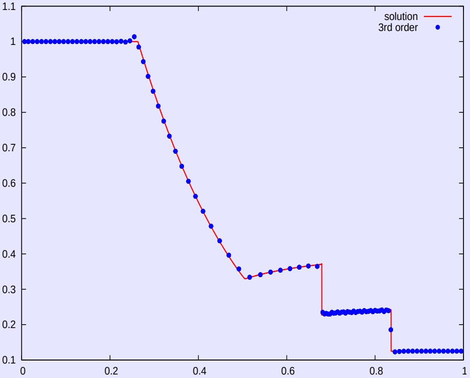

(b) Density profile.

FIGURE: Third-order DG solution for a Sod shock tube problem on a polar grid made of 100×3 cells.

Symmetry preservation

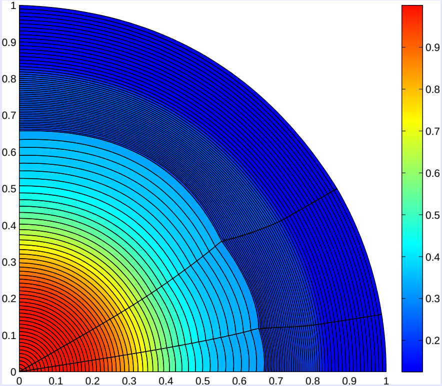

(a) First-order scheme.

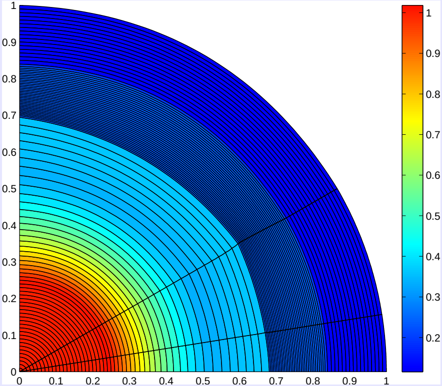

(b) Second-order scheme.

FIGURE: Sod shock tube problem on a polar grid made of 100 $\times$ 3 non-uniform cells.

Symmetry preservation

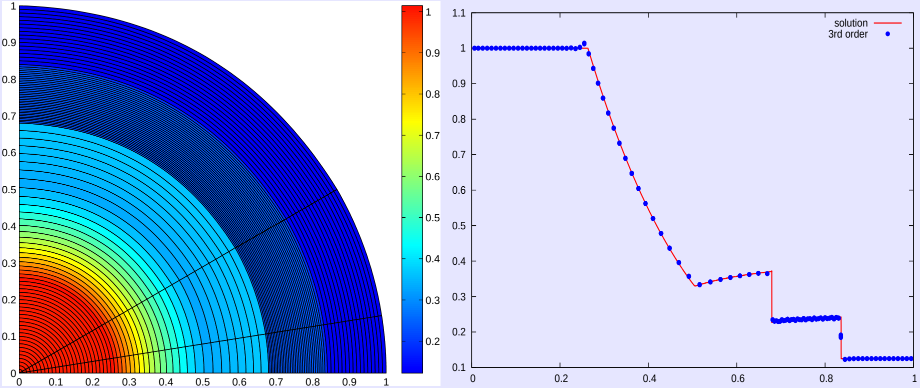

(a) Density map. (b) Density profile.

FIGURE: Third-order DG solution for a Sod shock tube problem on a polar grid made of 100 $\times$ 3 non-uniform cells.

Variant of the incompressible Gresho vortex problem

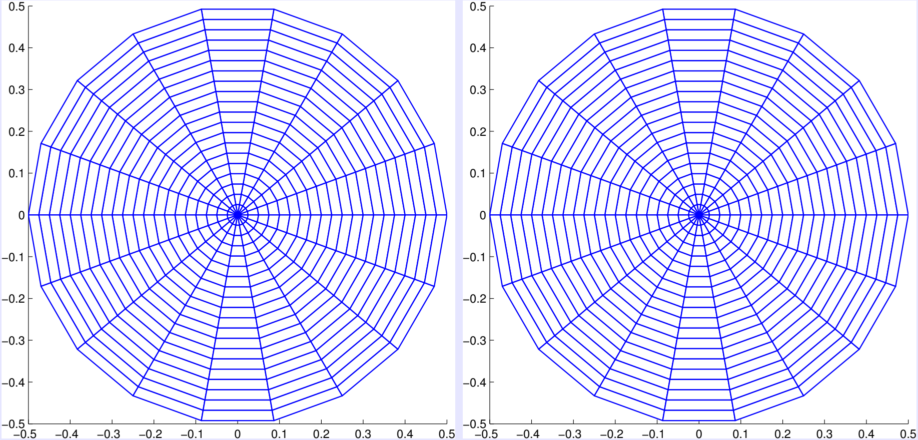

(a) First-order scheme.

(b) Second-order scheme.

FIGURE: Motion of a polar grid defined in polar coordinates by $(r, \theta) \in [0, 1] \times [0, 2\pi]$, with 40×18 cells at $t = 1$: zoom on the zone $(r, \theta) \in [0, 0.5] \times [0, 2\pi]$.

Numerical results

Variant of the incompressible Gresho vortex problem

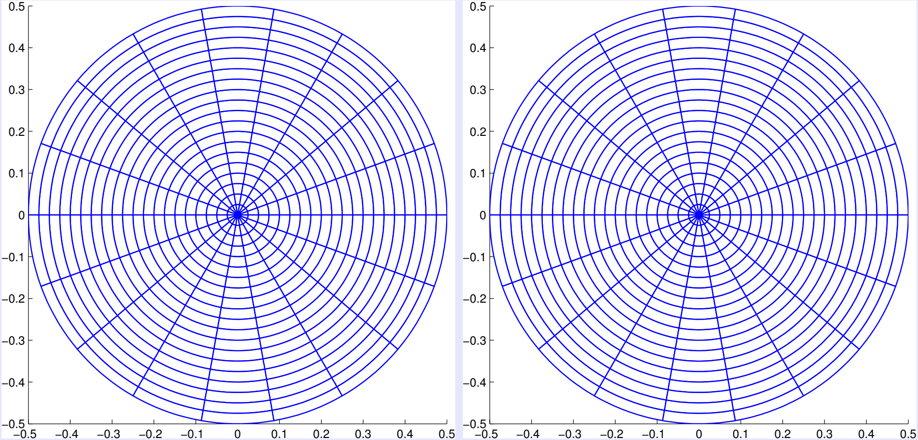

(a) Third-order scheme.

(b) Exact solution.

FIGURE: Motion of a polar grid defined in polar coordinates by $(r, \theta) \in [0, 1] \times [0, 2\pi]$, with 40×18 cells at $t = 1$: zoom on the zone $(r, \theta) \in [0, 0.5] \times [0, 2\pi]$.

Variant of the Gresho vortex problem

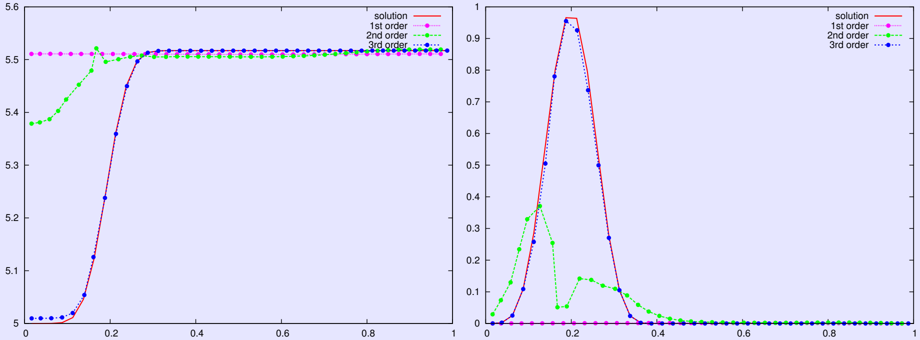

(a) Pressure profile.

(b) Velocity profile.

FIGURE: Gresho variant problem on a polar grid defined in polar coordinates by $(r, \theta) \in [0, 1] \times [0, 2\pi]$, with 40×18 cells at $t = 1$.

Numerical results

Variant of the Gresho vortex problem

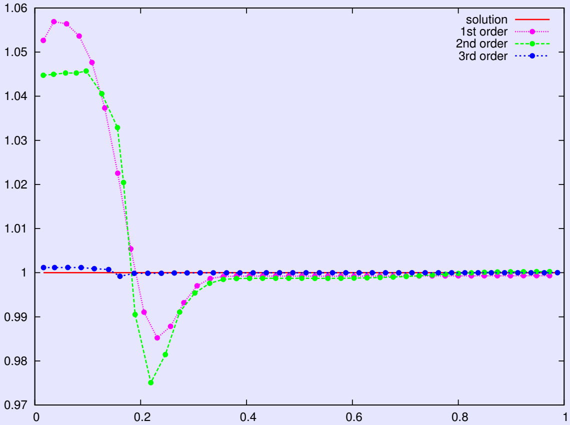

FIGURE: Gresho variant problem on a polar grid defined in polar coordinates by $(r, \theta) \in [0, 1] \times [0, 2\pi]$, with 40×18 cells at $t = 1$: density profile.

Kidder isentropic compression

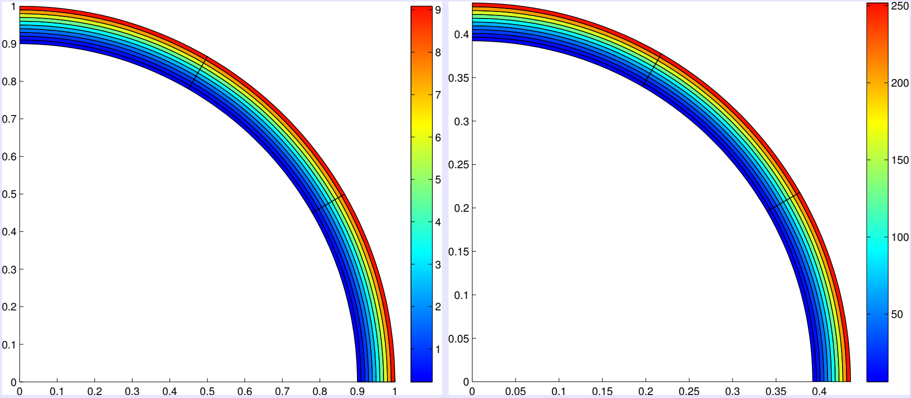

(a) At time $t = 0$. (b) At time $t = 0.9\tau$.

FIGURE: Third-order DG solution for a Kidder isentropic compression problem on a polar grid made of 10×3 cells: pressure map.

Numerical results

Kidder isentropic compression

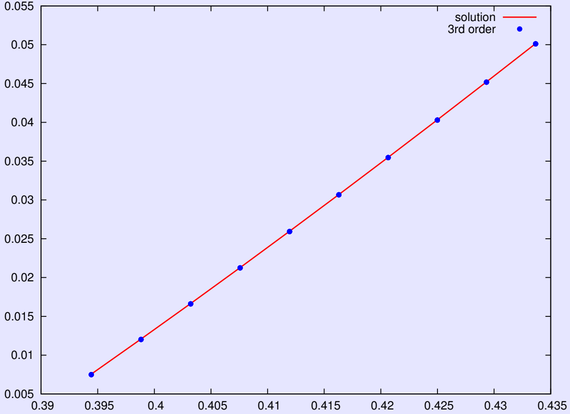

FIGURE: Third-order DG solution for a Kidder isentropic compression problem on a polar grid made of 10×3 cells: density profile.

Numerical results

Taylor-Green vortex problem

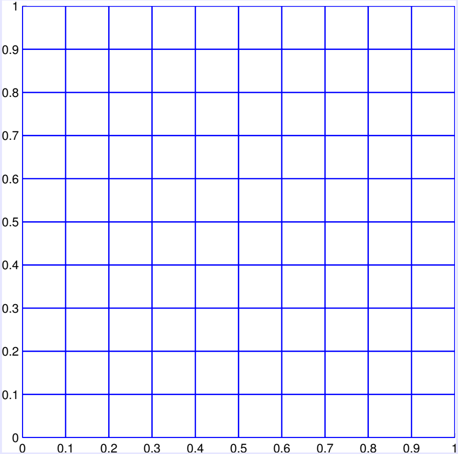

(a) Third-order scheme.

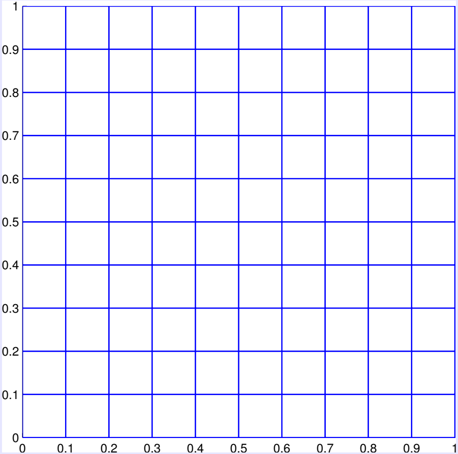

(b) Exact solution.

FIGURE: Motion of a 10×10 Cartesian mesh through a T.-G. vortex, at $t = 0.75$.

Rate of convergence computed on the pressure in the case of the Taylor-Green vortex

	L_1		L_2		L_∞	
h	$E^h_{L_1}$	$q^h_{L_1}$	$E^h_{L_2}$	$q^h_{L_2}$	$E^h_{L_\infty}$	$q^h_{L_\infty}$
$\frac{1}{10}$	2.50E-2	1.48	3.71E-2	1.30	1.72E-1	1.35
$\frac{1}{20}$	8.98E-3	1.88	1.51E-2	1.75	6.73E-2	1.27
$\frac{1}{40}$	2.44E-3	1.94	4.48E-3	1.95	2.79E-2	1.68
$\frac{1}{80}$	6.36E-4	2.00	1.16E-3	2.00	8.68E-3	1.95
$\frac{1}{160}$	1.59E-4	2.01	2.90E-4	2.01	2.24E-3	2.01

TABLE: Second-order DG scheme without limitation at time $t = 0.6$.

	L_1		L_2		L_∞	
h	$E^h_{L_1}$	$q^h_{L_1}$	$E^h_{L_2}$	$q^h_{L_2}$	$E^h_{L_\infty}$	$q^h_{L_\infty}$
$\frac{1}{10}$	4.39E-3	3.00	7.73E-3	2.68	3.90E-2	1.93
$\frac{1}{20}$	5.50E-4	3.04	1.21E-3	3.10	1.03E-2	2.98
$\frac{1}{40}$	6.68E-5	2.91	1.40E-4	2.87	1.30E-3	2.66
$\frac{1}{80}$	8.90E-6	2.89	1.92E-5	2.83	2.11E-4	2.74
$\frac{1}{160}$	1.20E-6	-	2.70E-6	-	3.16E-5	-

TABLE: Third-order DG scheme without limitation at time $t = 0.6$.

Rate of convergence computed on the pressure in the case of the Taylor-Green vortex

	L_1		L_2		L_∞	
h	$E^h_{L_1}$	$q^h_{L_1}$	$E^h_{L_2}$	$q^h_{L_2}$	$E^h_{L_\infty}$	$q^h_{L_\infty}$
$\frac{1}{10}$	2.67E-4	2.96	3.36E-4	2.94	1.21E-3	2.86
$\frac{1}{20}$	3.43E-5	2.97	4.36E-5	2.96	1.66E-4	2.93
$\frac{1}{40}$	4.37E-6	2.99	5.59E-6	2.98	2.18E-5	2.96
$\frac{1}{80}$	5.50E-7	2.99	7.06E-7	2.99	2.80E-6	2.99
$\frac{1}{160}$	6.91E-8	-	8.87E-8	-	3.53E-7	-

TABLE: Third-order DG scheme without limitation at time $t = 0.1$.

Content

1 Introduction and preliminary results

2 2D Lagrangian hydrodynamics

3 DG discretization general framework

4 Second-order DG scheme

5 Third-order DG scheme

6 Conclusions and perspectives

Conclusions and perspectives

Conclusions

- DG schemes up to 3rd order
  - 1D and 2D scalar conservation laws on general unstructured grids
  - 1D systems of conservation laws
  - **2D gas dynamics system in a total Lagrangian formalism**
- **GCL and Piola compatibility condition ensured by construction**
- **Dramatic improvement of symmetry preservation by means of third-order DG scheme**

Perspectives

- **High-order limitation on curved geometries**
- Improvement in midpont solver definition
- Code parallelization
- Study on computational cost and time
- Development of a 3rd order DG scheme on moving mesh
- Extension to 3D
- Extension to ALE and solid dynamics

Articles

- F. Vilar, P.-H. Maire and R. Abgrall, *Cell-centered discontinuous Galerkin discretizations for two-dimensional scalar conservation laws on unstructured grids and for one-dimensional Lagrangian hydrodynamics.* Computers and Fluids, 2010.
- F. Vilar, *Cell-centered discontinuous Galerkin discretization for two-dimensional Lagrangian hydrodynamics.* Computers and Fluids, 2012.
- F. Vilar, P.-H. Maire and R. Abgrall, *Third order Cell-Centered DG scheme for Lagrangian hydrodynamics on general unstructured Bezier grids.* Article in preparation.

Thank you

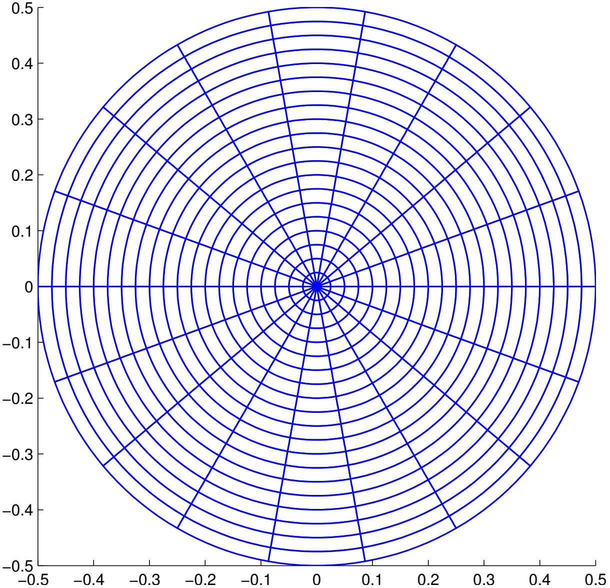

Third-order polynomial Taylor basis

Taylor expansion on the cell, located at the center of mass $\boldsymbol{\mathcal{X}}_c$

- $$\phi(\boldsymbol{X}) = \phi(\boldsymbol{\mathcal{X}}_c) + (X - \mathcal{X}_c)\frac{\partial \phi}{\partial X} + (Y - \mathcal{Y}_c)\frac{\partial \phi}{\partial Y} + \frac{1}{2}(X - \mathcal{X}_c)^2\frac{\partial^2 \phi}{\partial X^2} + (X - \mathcal{X}_c)(Y - \mathcal{Y}_c)\frac{\partial^2 \phi}{\partial X \partial Y} + \frac{1}{2}(Y - \mathcal{Y}_c)^2\frac{\partial^2 \phi}{\partial Y^2} + o(\|\boldsymbol{X} - \boldsymbol{\mathcal{X}}_c\|^2)$$

Polynomial basis functions

- $$\sigma_0^c = 1, \qquad \sigma_3^c = \frac{1}{2}\left[\left(\frac{X-\mathcal{X}_c}{\Delta X_c}\right)^2 - \left\langle\left(\frac{X-\mathcal{X}_c}{\Delta X_c}\right)^2\right\rangle_c\right],$$
  $$\sigma_1^c = \frac{X-\mathcal{X}_c}{\Delta X_c}, \qquad \sigma_4^c = \frac{(X-\mathcal{X}_c)(Y-\mathcal{Y}_c)}{\Delta X_c\,\Delta Y_c} - \left\langle\frac{(X-\mathcal{X}_c)(Y-\mathcal{Y}_c)}{\Delta X_c\,\Delta Y_c}\right\rangle_c,$$
  $$\sigma_2^c = \frac{Y-\mathcal{Y}_c}{\Delta Y_c}, \qquad \sigma_5^c = \frac{1}{2}\left[\left(\frac{Y-\mathcal{Y}_c}{\Delta Y_c}\right)^2 - \left\langle\left(\frac{Y-\mathcal{Y}_c}{\Delta Y_c}\right)^2\right\rangle_c\right].$$

Polynomial apprixation function components

- $\phi_0^c = \langle\phi\rangle_c$, $\phi_1^c = \Delta X_c \frac{\partial \phi}{\partial X}(\boldsymbol{\mathcal{X}}_c)$, $\phi_2^c = \Delta Y_c \frac{\partial \phi}{\partial Y}(\boldsymbol{\mathcal{X}}_c)$, $\phi_3^c = (\Delta X_c)^2 \frac{\partial^2 \phi}{\partial X^2}(\boldsymbol{\mathcal{X}}_c)$, $\phi_4^c = \Delta X_c\,\Delta Y_c \frac{\partial^2 \phi}{\partial X \partial Y}(\boldsymbol{\mathcal{X}}_c)$, $\phi_5^c = (\Delta Y_c)^2 \frac{\partial^2 \phi}{\partial Y^2}(\boldsymbol{\mathcal{X}}_c)$

Vertex-based hierarchical slope limiter

Third-order DG scheme limitation

- $\phi_h^c = \phi_0^c + c_1\left(\phi_1^c\sigma_1^c + \phi_2^c\sigma_2^c\right) + c_2\left(\phi_3^c\sigma_3^c + \phi_4^c\sigma_4^c + \phi_5^c\sigma_5^c\right)$

where c_1 and c_2 are the limiting coefficients

Linear reconstruction

- $\phi^{(1)} = \phi_0^c + c_1\left(\phi_1^c\,\frac{X-X_c}{\Delta X_c} + \phi_2^c\,\frac{Y-Y_c}{\Delta Y_c}\right)$
- $\phi_X^{(2)} = \Delta X_c\,\frac{\partial\,\phi_h^c}{\partial X} = \phi_1^c + c_X\left(\phi_3^c\,\frac{X-X_c}{\Delta X_c} + \phi_4^c\,\frac{Y-Y_c}{\Delta Y_c}\right)$
- $\phi_Y^{(2)} = \Delta Y_c\,\frac{\partial\,\phi_h^c}{\partial Y} = \phi_2^c + c_Y\left(\phi_4^c\,\frac{X-X_c}{\Delta X_c} + \phi_5^c\,\frac{Y-Y_c}{\Delta Y_c}\right)$

Limiting coefficient

- $c_2 = \min(c_X, c_Y)$
- $c_1 = \max(c_1, c_2)$

Smooth extrema preservation

Riemann invariants limitation

Riemann invariants differentials

- $\mathrm{d}\alpha_t = \mathrm{d}\boldsymbol{U}\,.\,\boldsymbol{t}$,
- $\mathrm{d}\alpha_- = \mathrm{d}P - \rho a\,\mathrm{d}\boldsymbol{U}\,.\,\boldsymbol{n}$,
- $\mathrm{d}\alpha_+ = \mathrm{d}P + \rho a\,\mathrm{d}\boldsymbol{U}\,.\,\boldsymbol{n}$,
- $\mathrm{d}\alpha_E = \mathrm{d}E - \boldsymbol{U}\,.\,\mathrm{d}\boldsymbol{U} + P\,\mathrm{d}(\frac{1}{\rho})$,

where $\boldsymbol{n}$ denotes a unit vector and $\boldsymbol{t} = \boldsymbol{e}_z \times \boldsymbol{n}$

Isentropic flow

- $\mathrm{d}P = -\rho^2 a^2\,\mathrm{d}(\frac{1}{\rho})$

New Riemann invariants differentials

- $\mathrm{d}\alpha_t = \mathrm{d}\boldsymbol{U}\,.\,\boldsymbol{t}$,
- $\mathrm{d}\alpha_- = \mathrm{d}(\frac{1}{\rho}) - \frac{1}{\rho a}\,\mathrm{d}\boldsymbol{U}\,.\,\boldsymbol{n}$,
- $\mathrm{d}\alpha_+ = \mathrm{d}(\frac{1}{\rho}) + \frac{1}{\rho a}\,\mathrm{d}\boldsymbol{U}\,.\,\boldsymbol{n}$,
- $\mathrm{d}\alpha_E = \mathrm{d}E - \boldsymbol{U}\,.\,\mathrm{d}\boldsymbol{U} + P\,\mathrm{d}(\frac{1}{\rho})$

2nd order DG discretization

DG discretization of the Lagrangian gas dynamics equations type

- $\mathsf{G}_i^c = (\mathsf{JF}^{-t})_i^c$ is constant on $\mathcal{T}_i^c$ and $\nabla_{\boldsymbol{X}} \sigma_q$ over Ω_c
- $$\int_{\Omega_c} \rho^0 \frac{\mathrm{d}\,\phi}{\mathrm{d}t} \sigma_q^c \,\mathrm{d}V = - \sum_{i=1}^{ntri} \mathsf{G}_i^c \nabla_X \sigma_q^c \,.\, \int_{\mathcal{T}_i^c} \boldsymbol{f} \,\mathrm{d}V + \sum_{p \in \mathcal{P}(c)} \int_p^{p^+} \overline{\boldsymbol{f}} \,.\, \sigma_q^c \,\mathsf{G}\boldsymbol{N} \mathrm{d}L$$
- $$\int_{\Omega_c} \rho^0 \frac{\mathrm{d}\,\psi}{\mathrm{d}t} \sigma_q^c \,\mathrm{d}V = - \sum_{i=1}^{ntri} \mathsf{G}_i^c \nabla_X \sigma_q^c \int_{\mathcal{T}_i^c} h \,\mathrm{d}V + \sum_{p \in \mathcal{P}(c)} \int_p^{p^+} \overline{h}\, \sigma_q^c \,\mathsf{G}\boldsymbol{N} \mathrm{d}L$$

Linear assumptions on face f_{pp^+}

- $\overline{\boldsymbol{f}}^{\,c}_{|_{pp^+}}(\zeta) = \boldsymbol{f}^+_{pc}\,(1-\zeta) + \boldsymbol{f}^-_{p^+c}\,\zeta$
- $\overline{h}^{\,c}_{|_{pp^+}}(\zeta) = h^+_{pc}\,(1-\zeta) + h^-_{p^+c}\,\zeta$

Linear property on face f_{pp^+}

- $\sigma^c_{q|_{pp^+}}(\zeta) = \sigma_q^c(\boldsymbol{X}_p)\,(1-\zeta) + \sigma_q^c(\boldsymbol{X}_{p^+})\,\zeta$

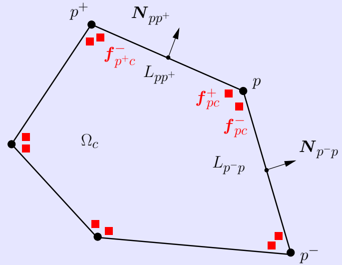

2nd order DG discretization

Analytical integration

- $\int_p^{p^+} \overline{\boldsymbol{f}} \sigma_q^c \,.\, \mathrm{G} \boldsymbol{N} \mathrm{d}L = \left(\int_0^1 \overline{\boldsymbol{f}}_{|_{pp^+}}(\zeta)\, \sigma^c_{q|_{pp^+}}(\zeta)\, \mathrm{d}\zeta \right) .\, \mathrm{G}_{|_{pp^+}} L_{pp^+} \boldsymbol{N}_{pp^+}$
- $\mathrm{G}_{|_{pp^+}} L_{pp^+} \boldsymbol{N}_{pp^+} = l_{pp^+} \boldsymbol{n}_{pp^+}$ Eulerian normal of face f_{pp^+}
- $\int_{\partial\Omega_c} \overline{\boldsymbol{f}}\, \sigma_q^c \,.\, \mathrm{G}\boldsymbol{N} \mathrm{d}L = \sum_{p \in \mathcal{P}(c)} \frac{1}{6} \left[\boldsymbol{f}^+_{pc} \,.\, (2\sigma_q^c(\boldsymbol{X}_p) + \sigma_q^c(\boldsymbol{X}_{p^+}))\, l_{pp^+} \boldsymbol{n}_{pp^+} \right.$ $\left. + \boldsymbol{f}^-_{p^+c} \,.\, (2\sigma_q^c(\boldsymbol{X}_{p^+}) + \sigma_q^c(\boldsymbol{X}_p)) l_{pp^+} \boldsymbol{n}_{pp^+} \right]$

Weighted corner normals

- $l^q_{pc} \boldsymbol{n}^q_{pc} = l^{-,q}_{pc} \boldsymbol{n}^{-,q}_{pc} + l^{+,q}_{pc} \boldsymbol{n}^{+,q}_{pc}$
- $l^{+,q}_{pc} \boldsymbol{n}^{+,q}_{pc} = \frac{1}{6} \left(2\sigma_q^c(\boldsymbol{X}_p) + \sigma_q^c(\boldsymbol{X}_{p^+})\right)\, l_{pp^+} \boldsymbol{n}_{pp^+}$
- $l^{-,q}_{pc} \boldsymbol{n}^{-,q}_{pc} = \frac{1}{6} \left(2\sigma_q^c(\boldsymbol{X}_p) + \sigma_q^c(\boldsymbol{X}_{p^-})\right)\, l_{p^-p} \boldsymbol{n}_{p^-p}$

2nd order DG discretization

Index permutation

- $\displaystyle\int_{\partial\Omega_c} \overline{\boldsymbol{f}}\,\sigma_q^c \,.\, \mathrm{G}\boldsymbol{N}\mathrm{d}L = \sum_{p\in\mathcal{P}(c)} \left(\boldsymbol{f}_{pc}^- \,.\, l_{pc}^{-,q}\boldsymbol{n}_{pc}^{-,q} + \boldsymbol{f}_{pc}^+ \,.\, l_{pc}^{+,q}\boldsymbol{n}_{pc}^{+,q} \right)$
- $\displaystyle\int_{\partial\Omega_c} \overline{h}\,\sigma_q^c \,\mathrm{G}\boldsymbol{N}\mathrm{d}L = \sum_{p\in\mathcal{P}(c)} \left(h_{pc}^- \, l_{pc}^{-,q}\boldsymbol{n}_{pc}^{-,q} + h_{pc}^+ \, l_{pc}^{+,q}\boldsymbol{n}_{pc}^{+,q} \right)$

Numerical fluxes on face f_{pp^+}

- $\overline{\boldsymbol{U}}^c_{|_{pp^+}}(\zeta) = \boldsymbol{U}_p\,(1-\zeta) + \boldsymbol{U}_{p^+}\,\zeta$
- $\overline{P}^c_{|_{pp^+}}(\zeta) = P_{pc}^+\,(1-\zeta) + P_{p^+c}^-\,\zeta$
- $\overline{P\boldsymbol{U}}^c_{|_{pp^+}}(\zeta) = (P\boldsymbol{U})_{pc}^+\,(1-\zeta) + (P\boldsymbol{U})_{p^+c}^-\,\zeta$

Fundamental assumption on face f_{pp^+}

- $\overline{P\,\boldsymbol{U}} = \overline{P}\,\overline{\boldsymbol{U}} \qquad \Longrightarrow \qquad (P\boldsymbol{U})_{pc}^- = P_{pc}^-\,\boldsymbol{U}_p$ and $(P\boldsymbol{U})_{pc}^+ = P_{pc}^+\,\boldsymbol{U}_p$

q^{th} moment of the subcell forces

- $\boldsymbol{F}_{pc}^q = P_{pc}^-\, l_{pc}^{-,q}\boldsymbol{n}_{pc}^{-,q} + P_{pc}^+\, l_{pc}^{+,q}\boldsymbol{n}_{pc}^{+,q}$

2nd order DG discretization

Semi-discrete equations GCL compatible

- $$\int_{\Omega_c} \rho^0 \frac{\mathrm{d}}{\mathrm{d}t}(\frac{1}{\rho})\sigma_q^c \,\mathrm{d}V = -\sum_{i=1}^{ntri} \mathrm{G}_i^c \nabla_X \sigma_q^c \cdot \int_{\mathcal{T}_i^c} \boldsymbol{U} \mathrm{d}V + \sum_{p \in \mathcal{P}(c)} \boldsymbol{U}_p \cdot l_{pc}^q \boldsymbol{n}_{pc}^q$$
- $$\int_{\Omega_c} \rho^0 \frac{\mathrm{d}\,\boldsymbol{U}}{\mathrm{d}t}\sigma_q^c \,\mathrm{d}V = \sum_{i=1}^{ntri} \mathrm{G}_i^c \nabla_X \sigma_q^c \int_{\mathcal{T}_i^c} P \mathrm{d}V - \sum_{p \in \mathcal{P}(c)} \boldsymbol{F}_{pc}^q$$
- $$\int_{\Omega_c} \rho^0 \frac{\mathrm{d}\,E}{\mathrm{d}t}\sigma_q^c \,\mathrm{d}V = \sum_{i=1}^{ntri} \mathrm{G}_i^c \nabla_X \sigma_q^c \cdot \int_{\mathcal{T}_i^c} P\,\boldsymbol{U} \mathrm{d}V - \sum_{p \in \mathcal{P}(c)} \boldsymbol{U}_p \cdot \boldsymbol{F}_{pc}^q$$

First moment equations

- $$m_c \frac{\mathrm{d}}{\mathrm{d}t}(\frac{1}{\rho})_0^c = \sum_{p \in \mathcal{P}(c)} \boldsymbol{U}_p \cdot l_{pc} \boldsymbol{n}_{pc}$$
- $$m_c \frac{\mathrm{d}\,\boldsymbol{U}_0^c}{\mathrm{d}t} = -\sum_{p \in \mathcal{P}(c)} \boldsymbol{F}_{pc}$$
- $$m_c \frac{\mathrm{d}\,E_0^c}{\mathrm{d}t} = -\sum_{p \in \mathcal{P}(c)} \boldsymbol{U}_p \cdot \boldsymbol{F}_{pc}$$

We recover the EUCCLHYD scheme

Compatibility of deformation gradient tensor discretization

Theoretical compatibility

- $\dfrac{\mathrm{d}\,\mathrm{F}}{\mathrm{d}t} = \nabla_X \boldsymbol{U}$
- $\dfrac{\mathrm{d}\,J}{\mathrm{d}t} = \dfrac{\partial}{\partial \mathrm{F}}(\det \mathrm{F}) : \dfrac{\mathrm{d}\,\mathrm{F}}{\mathrm{d}t} = (\det \mathrm{F})\mathrm{F}^{-\mathrm{t}} : \dfrac{\mathrm{d}\,\mathrm{F}}{\mathrm{d}t} = J\mathrm{F}^{-\mathrm{t}} : \dfrac{\mathrm{d}\,\mathrm{F}}{\mathrm{d}t}$
- $\dfrac{\mathrm{d}\,J}{\mathrm{d}t} = J\mathrm{F}^{-\mathrm{t}} : \nabla_X \boldsymbol{U} = J\mathrm{F}^{-\mathrm{t}} : (\nabla_x \boldsymbol{U})\,(\nabla_X \boldsymbol{x}) = J\mathrm{F}^{-\mathrm{t}}\mathrm{F}^{\mathrm{t}} : \nabla_x \boldsymbol{U}$
  $= J\,\mathrm{tr}(\nabla_x \boldsymbol{U}) = J\nabla_x \cdot \boldsymbol{U} = \nabla_X \cdot (J\mathrm{F}^{-1}\boldsymbol{U}) = \nabla_X \cdot (\mathrm{G}^{\mathrm{t}}\boldsymbol{U})$
- $\dfrac{\mathrm{d}\,J}{\mathrm{d}t} = \dfrac{\mathrm{d}}{\mathrm{d}t}\left(\dfrac{\rho^0}{\rho}\right) = \rho^0 \dfrac{\mathrm{d}}{\mathrm{d}t}\left(\dfrac{1}{\rho}\right) = \nabla_X \cdot (\mathrm{G}^{\mathrm{t}}\boldsymbol{U})$

Second-order discretizations compatibility

- $\dfrac{\mathrm{d}\,J_i^c}{\mathrm{d}t} = \mathrm{G}_i^c : \dfrac{\mathrm{d}\,\mathrm{F}_i^c}{\mathrm{d}t} = \dfrac{1}{|\mathcal{T}_i^c|} \sum_{p \in \mathcal{P}(\mathcal{T}_i)} \boldsymbol{U}_p \cdot \mathrm{G}_i^c L_{pi} \boldsymbol{N}_{pi} = \dfrac{1}{|\mathcal{T}_i^c|} \sum_{p \in \mathcal{P}(\mathcal{T}_i^c)} \boldsymbol{U}_p \cdot l_{pi} \boldsymbol{n}_{pi}$
- $\dfrac{\mathrm{d}\,J_i^c}{\mathrm{d}t} = \dfrac{\mathrm{d}}{\mathrm{d}t}\left(\dfrac{|\tau_i^c|}{|\mathcal{T}_i^c|}\right)$ thus $\left(\dfrac{1}{\rho}\right)_0^c = \dfrac{|\omega_c|}{m_c} = \dfrac{1}{m_c}\sum_{i=1}^{ntri} |\tau_i^c| = \dfrac{1}{m_c}\sum_{i=1}^{ntri} |\mathcal{T}_i^c|\, J_i^c$

3rd order DG discretization

DG discretization of the Lagrangian gas dynamics equations type

- $$\int_{\Omega_c} \rho^0 \frac{\mathrm{d}\,\phi}{\mathrm{d}t} \sigma_q^c \,\mathrm{d}V = -\sum_{i=1}^{ntri} \int_{\mathcal{T}_i^c} \mathsf{G}\,\nabla_X \sigma_q^c \,\boldsymbol{.}\, \boldsymbol{f}\,\mathrm{d}V + \sum_{p \in \mathcal{P}(c)} \int_p^{p^+} \overline{\boldsymbol{f}} \,\boldsymbol{.}\, \sigma_q^c \,\mathsf{G}\boldsymbol{N}\mathrm{d}L$$
- $$\int_{\Omega_c} \rho^0 \frac{\mathrm{d}\,\psi}{\mathrm{d}t} \sigma_q^c \,\mathrm{d}V = -\sum_{i=1}^{ntri} \int_{\mathcal{T}_i^c} \mathsf{G}\,\nabla_X \sigma_q^c \; h\,\mathrm{d}V + \sum_{p \in \mathcal{P}(c)} \int_p^{p^+} \overline{h}\, \sigma_q^c \,\mathsf{G}\boldsymbol{N}\mathrm{d}L$$

Quadratic assumptions on face f_{pp^+}

- $$\boldsymbol{f}_{|_{pp^+}}(\zeta) = (1-\zeta)(1-2\zeta)\,\boldsymbol{f}_{pc}^{+} + 4\zeta(1-\zeta)\,\boldsymbol{f}_{mc} + \zeta(2\zeta-1)\,\boldsymbol{f}_{p^+c}^{-}$$
- $$h_{|_{pp^+}}(\zeta) = (1-\zeta)(1-2\zeta)\,h_{pc}^{+} + 4\zeta(1-\zeta)\,h_{mc} + \zeta(2\zeta-1)\,h_{p^+c}^{-}$$

Linear and quadratic properties on face f_{pp^+}

- $$\mathsf{G}\,\boldsymbol{N}\,\mathrm{d}L_{|_{pp^+}}(\zeta) = \boldsymbol{n}\,\mathrm{d}l_{|_{pp^+}}(\zeta) = 2\left((1-\zeta)\,l_{pQ}\boldsymbol{n}_{pQ} + \zeta\, l_{Qp^+}\boldsymbol{n}_{Qp^+}\right)\mathrm{d}\zeta$$
- $$\sigma^c_{q|_{pp^+}}(\zeta) = (1-\zeta)(1-2\zeta)\,\sigma_q^c(\boldsymbol{X}_p) + 4\zeta(1-\zeta)\,\sigma_q^c(\boldsymbol{X}_m) + \zeta(2\zeta-1)\,\sigma_q^c(\boldsymbol{X}_{p^+})$$

3rd order DG discretization

Analytical integration + Index permutation

- $$\int_{\partial\Omega_c} \overline{\boldsymbol{f}} \sigma_q^c . \mathrm{G}\boldsymbol{N} \mathrm{d}L = \sum_{p \in \mathcal{P}(c)} \frac{1}{3} \left(\boldsymbol{f}_{pc}^- . \, l_{pc}^{-,q} \boldsymbol{n}_{pc}^{-,q} + \boldsymbol{f}_{pc}^+ . \, l_{pc}^{+,q} \boldsymbol{n}_{pc}^{+,q} \right) + \sum_{m \in \mathcal{M}(c)} \frac{2}{3} \boldsymbol{f}_{mc} . l_{mc}^q \boldsymbol{n}_{mc}^q$$
- $$\int_{\partial\Omega_c} \overline{h} \sigma_q^c \mathrm{G}\boldsymbol{N} \mathrm{d}L = \sum_{p \in \mathcal{P}(c)} \frac{1}{3} \left(h_{pc}^- \, l_{pc}^{-,q} \boldsymbol{n}_{pc}^{-,q} + h_{pc}^+ \, l_{pc}^{+,q} \boldsymbol{n}_{pc}^{+,q} \right) + \sum_{m \in \mathcal{M}(c)} \frac{2}{3} h_{mc} \, l_{mc}^q \boldsymbol{n}_{mc}^q$$

Weighted midpoint and corner normals

$$l_{mc}^q \boldsymbol{n}_{mc}^q = l_{mc}^{-,q} \boldsymbol{n}_{mc}^{-,q} + l_{mc}^{+,q} \boldsymbol{n}_{mc}^{+,q} \quad \text{and} \quad l_{pc}^q \boldsymbol{n}_{pc}^q = l_{pc}^{-,q} \boldsymbol{n}_{pc}^{-,q} + l_{pc}^{+,q} \boldsymbol{n}_{pc}^{+,q}$$

$$l_{mc}^{-,q} \boldsymbol{n}_{mc}^{-} = \frac{1}{5} \left(4\, \sigma_q^c(\boldsymbol{X}_m) + \sigma_q^c(\boldsymbol{X}_p) \right) l_{pQ} \boldsymbol{n}_{pQ}$$

$$l_{mc}^{+,q} \boldsymbol{n}_{mc}^{+} = \frac{1}{5} \left(4\, \sigma_q^c(\boldsymbol{X}_m) + \sigma_q^c(\boldsymbol{X}_{p^+}) \right) l_{Qp^+} \boldsymbol{n}_{Qp^+}$$

$$l_{pc}^{-,q} \boldsymbol{n}_{pc}^{-,q} = \frac{1}{10} \left[(6\, \sigma_q^c(\boldsymbol{X}_p) + 4\, \sigma_q^c(\boldsymbol{X}_{m^-})) l_{Q^-p} \boldsymbol{n}_{Q^-p} + (\sigma_q^c(\boldsymbol{X}_p) - \sigma_q^c(\boldsymbol{X}_{p^-})) l_{p^-p} \boldsymbol{n}_{p^-p} \right]$$

$$l_{pc}^{+,q} \boldsymbol{n}_{pc}^{+,q} = \frac{1}{10} \left[(6\, \sigma_q^c(\boldsymbol{X}_p) + 4\, \sigma_q^c(\boldsymbol{X}_m)) l_{pQ} \boldsymbol{n}_{pQ} + (\sigma_q^c(\boldsymbol{X}_p) - \sigma_q^c(\boldsymbol{X}_{p^+})) l_{pp^+} \boldsymbol{n}_{pp^+} \right]$$

3rd order DG discretization

Semi-discrete equations GCL compatible

$$\int_{\Omega_c} \rho^0 \frac{\mathrm{d}}{\mathrm{d}t}\left(\frac{1}{\rho}\right)\sigma_q^c \,\mathrm{d}V = -\sum_{i=1}^{ntri}\int_{\mathcal{T}_i^c} \boldsymbol{U}\,.\,\mathrm{G}\nabla_X \sigma_q^c \mathrm{d}V + \sum_{p\in\mathcal{P}(c)} \frac{1}{3}\boldsymbol{U}_p\,.\,l_{pc}^q \boldsymbol{n}_{pc}^q + \sum_{m\in\mathcal{M}(c)} \frac{2}{3}\boldsymbol{U}_m\,.\,l_{mc}^q \boldsymbol{n}_{mc}^q$$

$$\int_{\Omega_c} \rho^0 \frac{\mathrm{d}\boldsymbol{U}}{\mathrm{d}t}\sigma_q^c \,\mathrm{d}V = \sum_{i=1}^{ntri}\int_{\mathcal{T}_i^c} P\mathrm{G}\nabla_X \sigma_q^c \mathrm{d}V - \sum_{p\in\mathcal{P}(c)} \frac{1}{3}\boldsymbol{F}_{pc}^q - \sum_{m\in\mathcal{M}(c)} \frac{2}{3}\boldsymbol{F}_{mc}^q$$

$$\int_{\Omega_c} \rho^0 \frac{\mathrm{d}E}{\mathrm{d}t}\sigma_q^c \,\mathrm{d}V = -\sum_{i=1}^{ntri}\int_{\mathcal{T}_i^c} P\boldsymbol{U}\,.\,\mathrm{G}\nabla_X \sigma_q^c \mathrm{d}V + \sum_{p\in\mathcal{P}(c)} \frac{1}{3}\boldsymbol{U}_p\,.\,\boldsymbol{F}_{pc}^q + \sum_{m\in\mathcal{M}(c)} \frac{2}{3}\boldsymbol{U}_m\,.\,\boldsymbol{F}_{mc}^q$$

Equation on the first moment of the specific volume

- $$\int_{\partial\Omega_c} \overline{\boldsymbol{U}}\,.\,\mathrm{G}\boldsymbol{N}\mathrm{d}L = \sum_{p\in\mathcal{P}(c)} \frac{1}{3}\boldsymbol{U}_p\,.\,l_{Q^-Q}\boldsymbol{n}_{Q^-Q} + \sum_{m\in\mathcal{M}(c)} \frac{2}{3}\boldsymbol{U}_m\,.\,l_{pp^+}\boldsymbol{n}_{pp^+}$$

B. Boutin, E. Deriaz, P. Hoch, P. Navaro, *Extension of ALE methodology to unstructured conical meshes*, ESAIM: Proceedings, 2011

Rate of convergence computed on the pressure in the case of the Taylor-Green vortex

D.O.F	N	$E^h_{L_1}$	$E^h_{L_2}$	$E^h_{L_\infty}$	time (sec)
600	24×25	2.67E-2	3.31E-2	8.55E-2	2.01
2400	48×50	1.36E-2	1.69E-2	4.37E-2	11.0

TABLE: First-order DG scheme at time $t = 0.1$.

D.O.F	N	$E^h_{L_1}$	$E^h_{L_2}$	$E^h_{L_\infty}$	time (sec)
630	14×15	2.76E-3	3.33E-3	1.07E-2	2.77
2436	28×29	7.52E-4	9.02E-4	2.73E-3	11.3

TABLE: Second-order DG scheme without limitation at time $t = 0.1$.

D.O.F	N	$E^h_{L_1}$	$E^h_{L_2}$	$E^h_{L_\infty}$	time (sec)
600	10×10	2.67E-4	3.36E-4	1.21E-3	4.00
2400	20×20	3.43E-5	4.36E-5	1.66E-4	30.6

TABLE: Third-order DG scheme without limitation at time $t = 0.1$.

Sedov point blast problem on a Cartesian grid

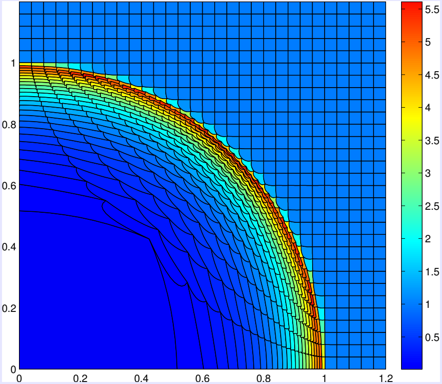

(a) Third-order scheme.

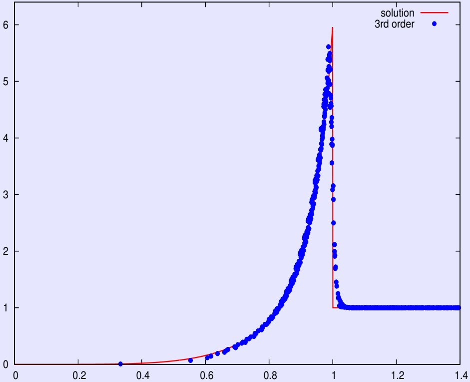

(b) Density profile.

FIGURE: Point blast Sedov problem on a Cartesian grid made of 30 $\times$ 30 cells: density.